PLASMA PHYSICS GROUP

Laminar Wave Train Structure of Collisionless Magnetic Slow Shocks

by

F. V. Coroniti

September, 1970

R-76

Laminar Wave Train Structure of Collisionless Magnetic Slow Shocks

by

F. V. Coroniti

September, 1970 R-76

Plasma Physics Group
Department of Physics
University of California
Los Angeles, California 90024

ABSTRACT

The laminar wave train structure of collisionless magnetic slow shocks is investigated using two fluid hydromagnetics with ion cyclotron radius dispersion. For shock strengths less than the maximally strong switch-off shock, in the shock leading edge dispersive steepening forms a magnetic field gradient, while in the downstream flow dispersive propagation forms a trailing wave train; dispersion scale lengths are the ion inertial length if $\beta < 1$ and the ion cyclotron radius if $\beta > 1$. In the switch-off slow shock leading edge, dispersion only produces rotations of the magnetic field direction; the gradient of the magnetic field magnitude, and hence the shock steepening length, is determined solely by resistive diffusion. The switch-off shock structure consists of a long trailing train of magnetic rotations which are gradually damped by resistivity. The low-β parallel fast switch-on shock has a similar wave train structure with the magnitude of the field rotations gradually increasing toward the downstream flow.

1.0 Introduction

A curious anomaloy in the collisionless shock literature is that very little is known theoretically about the structure of magnetic slow shocks. Collisionless fast shocks have been extensively investigated in both the limit that plasma dynamics are describable as a fluid [Refs. 1,2] and in the fully turbulent dissipative limit [Refs. 3-5]. Collisionless slow shock efforts have been confined to the parallel propagating low-β electrostatic ion acoustic shock in which the magnetic field is unimportant [Refs. 6-8]. Yet collisionless magnetic slow shocks, i.e., slow shocks in which the magnetic field dominates the shock structure, are of fundamental importance in space and cosmological plasmas. For example, Petschek's [9] theory of magnetic field annihilation, which has been applied to solar flares, magnetospheric convection [10], and quasars [11], involves magnetic slow shocks which stand upstream from the neutral sheet and provide most of the magnetic field dissipation.

As an initial effort this paper investigates the fluid or laminar wave train structure of both high- and low-β magnetic slow shocks. Historically, treating the plasma as a fluid has produced considerable knowledge of the internal macroscopic shock structure. In addition, the shock fluid dynamics have often provided insight into the collisionless microscopic turbulence required to generate shock dissipation [1]. Therefore, although laminar wave trains do not represent the final state of a collisionless shock theory, they often form a foundation upon which a unified shock theory can be constructed.

Before discussing collisionless slow shocks, a brief review of hydromagnetic slow shocks is both instructive and useful in motivating several of

the approximations employed in the collisionless analysis. The shock evolutionary conditions restrict the upstream slow shock flow velocity to be less than or equal to the intermediate C_I and greater than the slow C_{SL} hydromagnetic wave phase speeds (see Figure 1). In low-β plasmas the parallel and moderate to strong oblique slow shocks have supersonic upstream flow velocities. Although across all oblique slow shocks the magnetic field strength is reduced below the upstream value [12], for supersonic slow shocks the magnetic field change is small compared to the change in thermal pressure; hence the shock structure should be primarily electrostatic. Furthermore, in hydromagnetic or collisional plasmas, Coroniti [13] has shown that the dissipation in supersonic slow shocks is predominantly viscous. Oblique slow shocks whose upstream flow speed is less than the sound speed have large magnetic changes across the shock; the dissipated magnetic energy is divided between thermal and directed flow energy. Hence the shock structure should be dominately governed by the magnetic field. These subsonic magnetic slow shocks constitute the subject of this paper. (Note from Figure 1 that all $\beta > 1$ slow shocks are subsonic.) Finally, in MHD magnetic slow shocks resistivity alone is sufficient to provide the shock dissipation required by the Rankine-Hugoniot relations [13]. Therefore in the collisionless analysis, only an anomalous resistivity or turbulent electron-ion collisions will be included to simulate shock dissipation. Thermal conduction may contribute to the shock dissipation, but except for very weak slow shocks, it cannot provide all of the required dissipation [13].

In the collisionless or weak dissipation limit, the fluid shock structure is described by a coherent train of laminar wave oscillations. These wave trains consist of dispersively propagating waves on the same dispersion branch as the shock which phase stand in either the upstream or downstream

flow. The shock spatial scale lengths are governed by that dispersive length which permits the wave phase speed to equal the local flow velocity. Section 2.1 argues that for low-β oblique slow shocks, the ion inertial length should dominate the shock structure. The large magnetic energy dissipation across strong low-β magnetic slow shocks, however, implies that the downstream flow will be moderate to high-β. Here and in all high-β slow shocks ion cyclotron radius dispersion is competitive with or even dominates ion inertial dispersion, and must be included in the wave train structure.

The appropriate fluid equations for the slow shock analysis, therefore, are Chew-Goldberger-Low hydromagnetics with first order ion cyclotron radius corrections [14]. This fluid system, however, contains several difficulties when applied to collisionless shocks. First, a complete set of Rankine-Hugoniot conservation relations does not exist for oblique shocks since the parallel and perpendicular pressures are not independently specified [15,16] (Section 2.3). Second, the heat flow along the magnetic field is not determined by the fluid moments (Section 2.4). The resolution of both these difficulties requires previous knowledge of the plasma turbulent dissipation. Since the slow shock turbulence structure is beyond the scope of this initial paper, two assumptions will be made to permit utilization of these fluid equations: the pressure anisotropy and the parallel heat flow are assumed to be small and to make negligible contribution to the shock structure.

In Section 3.0 the differential equation which describes the wave train spatial structure is analyzed by employing the standard technique of linearization about the upstream and downstream Rankine-Hugoniot stationary flows [2]. The linearized wave train differential equation is unambiguously applicable to weak and moderate strength slow shocks, i.e., shocks with upstream flow velocities less than the intermediate wave speed. Maximum

strength or switch-off slow shocks whose upstream flow velocity equals the intermediate speed require special consideration and are analyzed in Section 4.0. The results of Section 3.0 are that ion inertial dispersion for low-β and ion cyclotron radius dispersion for high-β produce wave trains which trail in the downstream flow behind the shock leading edge.

In Section 4.0 the nonlinear wave train differential equations for oblique low-β switch-off slow shocks are derived; only ion inertial dispersion is retained. The switch-off shock is found to steepen only if the leading edge is dissipative. The switch-off shock wave train structure is a long trailing train of magnetic field rotations with ion inertia oscillation length; starting at the upstream point the magnetic field magnitude is gradually damped by resistivity in a scale length greatly exceeding the ion inertia length. The linearized wave train solutions of Section 3.0 are then reconsidered in the switch-off shock limit, and are found to be consistent with the results from the nonlinear switch-off shock analysis. Parallel low-β fast switch-on shocks obey the same nonlinear equations as slow switch-off shocks, and hence have a similar wave train structure.

2.0 The Dispersive Hydromagnetic Equations

2.1 Dispersive Scale Lengths

Since collisionless hydromagnetics contain neither a basic length or time scale, shocks and discontinuities are infinitely thin surfaces across which the plasma state changes discontinuously. In order to resolve the spatial structure of the shock, hydromagnetics must be generalized to include short scale length plasma dispersion. In two fluid hydromagnetic theory, the finite mass of ions and electrons is reflected by the inertial scale lengths C/ω_{p_+} and C/ω_{p_-}. (C is the light speed, $\omega_{p_\pm} = (4\pi Ne^2/M_\pm)^{1/2}$ is the specie ($\pm$) plasma frequency, N is the number density, e the electronic charge, and $M_\pm$ the ion or electron mass. Gaussian units are used throughout.) For moderate or high temperature plasmas, the finite cyclotron radius (FCR) $R_\pm = C_\pm/\Omega_\pm$ of the gyrating particles introduces further dispersive lengths. ($C_\pm = (T^\pm/M_\pm)^{1/2}$ is the specie thermal speed, $T^\pm$ the temperature in energy units, and $\Omega_\pm = eB/M_\pm C$ is the gyration frequency in a magnetic field of strength B.) In addition charge separation between ions and electrons results in Debye length, $\lambda_{D_\pm} = C_\pm/\omega_{p_\pm}$ dispersion. A useful scaling relation between inertial and FCR dispersion lengths is $R_\pm \sim \sqrt{\beta_\pm}\ C/\omega_{p_\pm}$ where $\beta_\pm = 8\pi NT^\pm/B^2$. Therefore if $\beta^\pm << 1$ inertial dispersion generally dominates the shock structure, whereas if $\beta^\pm > 1$ FCR dispersion is important.

The selection of which dispersion lengths influence the structure of slow shocks can be motivated from the theory of linear wave propagation. In a collisionless plasma the limitation of shock steepening is accomplished by the dispersive propagation of waves out of the shock front. A steady state

is established when the compressive energy going into shock steepening is balanced by the loss of energy from wave propagation [1]. With the addition of dissipation, the shock structure takes the form of a leading (trailing) wave train if dispersion increases (decreases) the linear wave phase speed. The shock "thickness" or structure is essentially determined by the wave dispersion scale length.

In the linear two fluid theory, which does not include FCR corrections, the dispersion relation for the slow wave propagating at a large angle to the DC magnetic field is approximately [17,18]

$$\frac{\omega^2}{k^2} = C_{SL}^2 \left[1 - \frac{k^2 C^2}{\omega_{p_+}^2} \frac{C_I^2}{C_F^2} \frac{C_S^2 - C_{SL}^2}{C_I^2 - C_{SL}^2} \right] \tag{2.1}$$

$C_I = C_A \cos\theta$ is the intermediate hydromagnetic speed, $C_A = B/(4\pi N M_+)^{1/2}$ is the Alfven speed, θ is the angle between $\underline{K}$ and $\underline{B}$, $C_S = (\gamma P/\rho)^{1/2}$ is the sound speed with γ the ratio of specific heats, P the pressure, and ρ the mass density. The hydromagnetic fast C_F and slow C_{SL} speeds are defined as

$$\left.\begin{matrix} C_F^2 \\ C_{SL}^2 \end{matrix}\right\} = \frac{C_A^2 + C_S^2}{2} \pm \left[\left(\frac{C_A^2 + C_S^2}{2} \right)^2 - C_I^2 C_S^2 \right]^{1/2} \tag{2.2}$$

In (2.1), $kC/\omega_{p_+} < 1$ was assumed. Since $C_S > C_{SL}$ and $C_I > C_{SL}$, ion inertia reduces the slow wave phase velocity below the hydromagnetic speed. If $\beta_+ > 1$, Coroniti and Kennel [19] found that ion cyclotron radius (ICR) dispersion also decreases the slow wave phase speed.

For propagation parallel to the magnetic field and $\beta_\pm < 1$ the slow wave is the ion acoustic mode with the dispersion relation [17]

$$\frac{\omega^2}{k^2} = \frac{C_S^2}{1 + k^2\lambda_D^2} \tag{2.3}$$

Here the slow wave is electrostatic and remains non-dispersive until $k\lambda_D \sim 1$. The ion acoustic electrostatic shock has received considerable study using both fluid equations [6,8] and the Vlasov equation [7]. Therefore this paper will restrict consideration to magnetic slow shocks, i.e., shock propgation at large angles to the magnetic field for both high- and low-β and near parallel propagation for $\beta > 1$ so that $C_S > U$. (Note that for $\theta = 0$ and $\beta > 1$ the intermediate and slow wave speeds are equal; therefore from the shock evolutionary conditions [12] the slow shock is of zero strength.) For $\beta >> 1$ and $\theta << 1$, the slow wave dispersion relation with ICR corrections for $kR_+ < 1$ is [20]

$$\frac{\omega^2}{k^2} = C_{SL}^2 \left[1 - k^2 R_+^2 \frac{P/\rho}{C_I^2 - C_{SL}^2} \right] \tag{2.4}$$

Hence for near-parallel propagation ICR dispersion reduces the slow wave speed.

For $kC/\omega_{p_+} >> 1$ the slow wave goes to a resonance at $\omega = \Omega_+ \cos\theta$ [21] and no additional dispersive scale lengths affect the wave. Therefore the spatial structure of magnetic slow shocks should be dominated by ion inertia and ICR dispersion lengths.

2.2 FCR - CGL Fluid Equations

The system of equations which will be employed to investigate the shock structure are the Chew-Goldberger-Low (CGL) hydromagnetic equations with first order ICR corrections as derived by MacMahon [14] from the moments

of the Vlasov equation. The ICR-CGL equations describe the plasma fluid behavior on scale lengths long compared to R_+ . The shock structure is assumed time independent in the co-moving shock frame and the planar shock is taken to propagate in the positive x-direction. The upstream (and downstream by the co-planarity theorem) magnetic field is assumed to be in the x-z plane, and all plasma quantities vary only in the x-direction.

With the above assumption there are three integrals of the motion which express conservation laws. The continuity of mass flow is given by

$$\rho U = \rho_1 U_1 \tag{2.5}$$

where U is the x-component of the fluid velocity and subscript (1) denotes upstream flow conditions. The three components of the vector momentum equation are

$$\rho U(U-U_1) + P^{(1)}_{xx} - P^{(1)}_{xx_1} + \frac{B_z^2 + B_y^2 - B_{z_1}^2}{8\pi} = 0 \tag{2.6}$$

$$\rho U V_y + P^{(1)}_{xy} - \frac{B_x B_y}{4\pi} = 0 \tag{2.7}$$

$$\rho U V_z + P^{(1)}_{xz} - P^{(1)}_{xz_1} - \frac{B_x(B_z-B_{z_1})}{4\pi} = 0 \tag{2.8}$$

V_y and V_z are the y and z components of the fluid velocity, respectively. $P^{(1)}_{xx}$, $P^{(1)}_{xy}$, and $P^{(1)}_{xz}$ are components of the pressure tensor $\underset{\approx}{P}^{(1)}$, and the superscript (1) in the notation of MacMahon [14] denotes the retention of first order ICR corrections. B_x , the normal component of $\underline{B}$, is, of course, constant. Note that $V_{y_1} = V_{z_1} = B_{y_1} = 0$.

Conservation of total energy is expressed by

$$\rho U\left[\frac{U^2+V_y^2+V_z^2}{2}\right]+U\left(P_{\perp}^{(1)}+\frac{1}{2}P_{\parallel}^{(1)}+P_{xx}^{(1)}\right)+V_yP_{xy}^{(1)}$$

$$+V_zP_{xz}^{(1)}-U_1\left(P_{\perp_1}^{(1)}+\frac{1}{2}P_{\parallel_1}^{(1)}+P_{xx_1}^{(1)}\right)+\frac{U_1B_{z_1}(B_z-B_{z_1})}{4\pi}$$

$$-\rho U\frac{U_1^2}{2}+\left(\underline{q}_{\parallel}^{\parallel(0)}+\underline{q}_{\parallel}^{\perp(0)}+\underline{q}_{\perp}^{\perp(1)}+\underline{q}_{\perp}^{\parallel(1)}\right)\cdot\hat{x}=0 \tag{2.9}$$

$P_{\perp}^{(1)}$ and $P_{\parallel}^{(1)}$ are the perpendicular and parallel to $\underline{B}$ components of the pressure tensor. $(\underline{q}_{\parallel}^{\parallel(0)}+\underline{q}_{\parallel}^{\perp(0)})\cdot\hat{x}$ is the zeroth order heat flow along $\hat{x}$ and $(\underline{q}_{\perp}^{\perp(1)}+\underline{q}_{\perp}^{\parallel(1)})\cdot\hat{x}$ is the first order ICR heat flow along $\hat{x}$. Complete expressions for the pressure tensor, $\underline{q}_{\perp}^{\perp(1)}$ and $\underline{q}_{\perp}^{\parallel(1)}$ can be found in MacMahon [14].

After substitution of Ampere's law, $\nabla\times\underline{B}=\frac{4\pi}{C}\underline{J}$, the two components of Ohm's law which describe the coupling between the fluid and the magnetic field become

$$\frac{C^2}{\omega_{p_-}^2}\frac{U}{U_1}\frac{d}{dx}\left(U\frac{dB_z}{dx}\right)+\frac{C^2}{\omega_{p_-}^2}\frac{\nu U}{U_1}\frac{dB_z}{dx}$$

$$-\frac{C}{\omega_{p_+}}\frac{C_IU}{U_1}\frac{dB_y}{dx}=UB_z-U_1B_{z_1}-V_zB_x \tag{2.10}$$

$$\frac{C^2}{\omega_{p_-}^2}\frac{U}{U_1}\frac{d}{dx}\left(U\frac{dB_y}{dx}\right)+\frac{C^2}{\omega_{p_-}^2}\frac{\nu U}{U_1}\frac{dB_y}{dx}$$

$$+\frac{C}{\omega_{p_+}}\frac{C_IU}{U_1}\frac{dB_z}{dx}=UB_y-V_yB_x \tag{2.11}$$

where $C_I=B_x/(4\pi\rho_1)^{1/2}$ and $\omega_{p_\pm}=(4\pi N_1e^2/M_\pm)^{1/2}$. The second order

derivative term represents electron inertial dispersion and has been retained for completeness. The terms multiplied by C/ω_{p_+} represent ion inertial dispersion, and these terms couple B_y and B_z. ν represents an ion-electron collision frequency, i.e., resistivity, and introduces irreversibility into the above equations; ν may arise from either weak Coulomb collisions or from anomalous turbulent dissipation.

The program for obtaining a differential equation which describes the shock spatial structure is to eliminate all of the plasma variables in terms of the magnetic field B_z and B_y. The above equations, however, are not in closed form. There is no equation which uniquely determines $P_{\parallel}^{(1)}$ and $P_{\perp}^{(1)}$, and the zeroth order heat flow is not specified. Furthermore, from the general equations of MacMahon [14], $P_{\parallel}^{(1)}$, $P_{\perp}^{(1)}$, $\underline{q}_{\perp}^{\perp(1)}$, and $\underline{q}_{\perp}^{\parallel(1)}$ depend on higher order than third moments of the Vlasov equation. In order to truncate the moment hierarchy, some approximations are needed and will be discussed in the following sections.

2.3 The Rankine-Hugoniot Relations

Some of the above difficulties could be removed if an adequate number of conservation relations were available. Before proceeding to the FLR-CGL equations, however, the significance of the Rankine-Hugoniot relations is best appreciated by reviewing hydromagnetic shocks. The hydromagnetic equations are a closed set of nonlinear hyperbolic partial differential equations; the Cauchy problem is, therefore, well posed, and the solution is obtainable by the method of characteristics [12]. The time independent hydromagnetic equations can be written in the form $\nabla \cdot \underline{j} = 0$ where $\underline{j}$ is the mass, momentum, or energy flux. Hence there exist three integrals of the motion which are the Rankine-Hugoniot conservation laws. The time

independent equations permit discontinuous changes in the characteristics with the final state determined from the initial one by the conservation laws. The significance for shocks is that no information about the internal structure and dissipation processes is required in order to specify the downstream state.

Now consider CGL hydromagnetics without ICR corrections. Assume that the characteristics of these equations are real; i.e., the conditions for the firehose or mirror instabilities are not satisfied, so that the shock flow can be assumed time independent. There are eight variables, ρ , $\underline{V}$, B_z , B_y , $P_{\parallel}^{(1)}$, and $P_{\perp}^{(1)}$ but only seven equations which are in the form of conservation laws [15,16].

It might be thought that this difficulty could be resolved by writing separate equations for the parallel and perpendicular energies. Within the CGL system the following two energy equations are obtained.

$$\nabla \cdot \left[\rho \underline{V} \left(\frac{U_{\perp}^2}{2} + \frac{P_{\perp}}{\rho} \right) + \underline{U}_{\perp} \cdot \underset{\approx}{P} + \frac{\underline{B} \times (\underline{V} \times \underline{B})}{4\pi} \right] + \rho U_{\parallel} \underline{U}_{\perp} \cdot \frac{d\hat{B}}{dt} = 0 \tag{2.12}$$

$$\nabla \cdot \left[\rho \underline{V} \left(\frac{U_{\parallel}^2}{2} + \frac{P_{\parallel}}{2\rho} \right) + \underline{U}_{\parallel} \cdot \underset{\approx}{P} \right] + - \rho U_{\parallel} U_{\perp} \cdot \frac{d\hat{B}}{dt} = 0 \tag{2.13}$$

where d/dt is the convective derivative. $\underline{U}_{\parallel}$ and $\underline{U}_{\perp}$ are the velocity components parallel and perpendicular to $\underline{B}$, respectively.

Except for perpendicular fast shocks in which $d\hat{B}/dt = 0$, the parallel and perpendicular energies are coupled. (For perpendicular shocks $U_{\parallel} = 0$ and (2.13) yields $P_{\parallel}/\rho = T_{\parallel}$ = constant. Although (2.12) also yields $P_{\perp}/\rho B$ = constant, Goldberg [22] has shown that $P_{\perp}/\rho B$ is not conserved to

first order in R_+ . Hence $T_{\parallel}$ = constant is the appropriate conservation law.) The coupling for oblique shocks arises from the centripedal acceleration of the plasma along the magnetic field due to variations in the field direction. Since the Vlasov equation always conserves total energy, changes in parallel energy must come, in part, at the expense of the perpendicular energy and vice versa. In hydromagnetics this coupling never occurs since the assumption of pressure isotropy implies that any gain in parallel energy is transferred back to perpendicular energy by collisions.

Since the parallel and perpendicular energies are coupled for oblique shocks in the lowest order CGL theory, the retention of first order FCR corrections cannot remove the coupling. In fact since FCR terms couple the various degrees of freedom, $P_\perp$ and $P_\parallel$ only become more entwined in the first order theory. Therefore neither CGL nor FCR-CGL hydromagnetics possesses a closed set of Rankine-Hugoniot relations for oblique shocks. Hence the downstream state is not uniquely determined by the upstream flow conditions but depends on the detailed dissipation processes within the shock front [15,16].

In a collisionless shock the pressure moments of the particles' kinetic equation, including the plasma turbulent "collision" operator which provides anomalous dissipation, would yield a relation between $P_\parallel$ and $P_\perp$ through the shock front. Since the kinetic theory of the plasma turbulence appropriate for slow shocks is far beyond the scope of this initial paper, the simplest approximation that completes the FCR-CGL equations will be made, i.e., the parallel and perpendicular pressures are assumed equal in the lowest and first order equations. In effect, the pressure anisotropy is taken to be of higher order in the ICR expansion than the ICR dispersive contributions. As shown in Section 3.0, ICR dispersion enters as $(R_+/L)^2$ where L is typical scale length for the shock; therefore the pressure anisotropy $P_\parallel - P_\perp / P_\parallel$

is assumed to be of order $(R_+/L)^3$. A word of caution is advisable, however. Anisotropy driven wave turbulence could constitute an important part of the slow shock structure, as it does for fast Alfven shocks [5] and is possible for finite-β whistler fast shocks [23]. In these fully turbulent shock flows, both the resonant and non-resonant anisotropy instabilities must be treated directly by the Vlasov-Maxwell equations, and such shocks, therefore, are *inherently not amenable to investigation by fluid equations.*

2.4 Heat Flow

Closure of the FCR-CGL hydromagnetic equations requires truncation of the moment hierarchy derived from the Vlasov equation. The zeroth order parallel heat flow, which arises from the third order moment, however, is not determined by the fluid moments [14]. The parallel heat flow depends on the detailed shape of the particles' distribution functions, and can only be specified for collisionless shocks when the kinetic turbulent "collision" operator is known. The usual argument used in CGL is that only a few collisions are needed to suppress the parallel heat flow. Since collisionless shocks must involve turbulent dissipation which replaces ordinary Coulomb collisions, the parallel heat flow will probably be suppressed within the shock layer. Every line of force must pass through the turbulent region in the shock layer so that if the heat flow is negligible there, it can also be neglected in the upstream and downstream flow. Furthermore, in the context of hydromagnetic shocks, Coroniti [13] has shown that heat flow dissipation acting alone can provide the required dissipation only for very weak fast and slow shocks. Hence for most shocks other types of dissipation such as resistivity and/or viscosity are necessary for a complete shock transition.

With the lack of a turbulent "collision" operator, for the purposes of this paper the effect of parallel heat flow on the structure of slow shocks will be neglected, thus closing the fluid equations. In addition fourth and higher order moments will also be neglected. Formally, this neglect is equivalent to assuming that the parallel heat flow, $(\underline{q}_{\parallel}^{\parallel(0)} + \underline{q}_{\perp}^{\perp(0)}) \cdot \hat{x}$ and higher moments are of order $(R_+/L)^3$. Again, a word of caution is advisable. Oblique shocks do have temperature gradients along the magnetic field, and there could exist a large heat flow directed upstream from the shock front which could greatly broaden the shock or might, in certain circumstances, render the whole concept of a shock transition meaningless. Section 5.0 comments further on the importance of parallel heat flow in magnetic slow shocks.

2.5 Summary

From the linear wave theory the spatial structure of magnetic slow shocks should be at the ion inertia length for $\beta < 1$ and the ICR length for $\beta > 1$. The FCR-CGL hydromagnetic equations, which are appropriate for describing the shock fluid structure, contain two difficulties: a complete set of conservation laws which relate $P_{\parallel}$ and $P_{\perp}$ and uniquely specify the downstream state does not exist for oblique shocks; the zeroth order parallel heat flow is not determined by the fluid moments so that the equations are not closed. The resolution of both difficulties requires a knowledge of the plasma turbulent dissipation in the shock. In order to continue with the investigation of the shock fluid structure without first solving the turbulent dissipation problem, two assumptions will be made: the parallel and perpendicular pressures are assumed equal to order $(R_+/L)^2$; the parallel heat flow and higher order moments are taken to be of order $(R_+/L)^3$, and hence neglected.

3.0 Fluid Dispersive Structure of Magnetic Slow Shocks

3.1 Introduction

With the above assumptions the ICR-CGL equations could be reduced to a coupled system of second order nonlinear differential equations which would describe the spatial variation of the magnetic field from the upstream to downstream state. Although of interest for numerical methods, the nonlinear wave train differential equations are usually too complex for solution by analytic methods. As with many nonlinear differential equations, however, the nature of the wave train solutions is obtainable by linearizing the differential equations about their stationary points. For shock wave trains, the stationary points are given by the spatially uniform asymptotic flow states which satisfy the Rankine-Hugoniot relations. A shock transition requires that the upstream (downstream) state be unstable (stable) to small linear perturbations. Although the linearization technique does not realize the nonlinear structure of the shock center, whenever numerical wave train solutions have been obtained, the results have confirmed the qualitative predictions based on linearization [2,24]. Therefore in this paper the structure of magnetic slow shocks will be investigated from the linearized wave train differential equations.

In Section 3.2 the linearized differential equations are derived and approximations applicable to magnetic slow shocks are developed. The low-β oblique slow shock is analyzed in Section 3.3 and is found to have a trailing ion inertia length wave train. Section 3.4 considers high-β slow shocks. Both oblique and at near-parallel propagating shocks have trailing ICR length wave trains.

3.2 Linearized Wave Train Differential Equations

At a Rankine-Hugoniot stationary point the plasma is spatially uniform so that all x-derivatives vanish; furthermore $V_y = B_y = 0$. The linearized differential equation is obtained by perturbing equations (2.6) - (2.11) about the stationary point and retaining only lowest order terms in the perturbed variables. The coefficients of all perturbed quantities are then to be evaluated at either the upstream or downstream stationary points.

After elimination of $\delta P_{xx}^{(1)} = \delta P^{(1)} + \delta T_{xx}$ (see Appendix A.2), δV_y , and δV_z , the linearized form of (2.6) - (2.9) can be reduced to the following equation for δU

$$\delta U = \frac{-1}{\rho(U^2-C_S^2)} \left[\frac{UB_z \delta B_z}{4\pi} + U\delta T_{xx} - \frac{2}{3} (\delta \underset{\sim}{q}_{\perp}^{(1)} + \delta \underset{\sim}{q}_{\perp}^{u(1)}) \cdot \hat{x} \right] \tag{3.1}$$

The sound speed is now defined as $C_S^2 = \frac{5}{3} \frac{p^{(1)}}{\rho}$. In deriving (3.1) pressure isotropy and neglect of zeroth order parallel heat flow are assumed. In addition, the relation $U_1 B_{z_1} = UB_z - [B_x^2 (B_z - B_{z_1})/4\pi\rho U]$, which follows from (2.8), (2.10), and (A.2.7) evaluated at a stationary point, was used to eliminate $U_1 B_{z_1}$ from the energy equation. δT_{xx} and $\delta(\underset{\sim}{q}_{\perp}^{(1)} + \underset{\sim}{q}_{\perp}^{u(1)}) \cdot \hat{x}$ are given by (A.2.6) and (A.2.9), respectively.

The coupled wave train differential equations are obtained from the linearized form of the Ohms law (2.10) and (2.11). After elimination of δU by (3.1), δV_y by (2.7), δV_z by (2.8), and substitution of the relations (A.2.5) - (A.2.9) which are derived in Appendix A.2, equations (2.10) and (2.11) become

$$D \frac{d^2 \delta B_z}{dx^2} + r_m \frac{d\delta B_z}{dx} - \frac{C}{\omega_{p_+}} \frac{C_I}{U} F \frac{d\delta B_y}{dx} = A_z \delta B_z \tag{3.2}$$

$$G\frac{d^2\delta B_y}{dx^2} + r_m\frac{d\delta B_y}{dx} + \frac{C}{\omega_{p_+}}\frac{C_I}{U}F\frac{d\delta B_z}{dx} = A_y\delta B_y \tag{3.3}$$

where

$$A_z = \frac{(U^2-C_F^2)(U^2-C_{SL}^2)}{U^2(U^2-C_S^2)} \tag{3.4}$$

$$A_y = 1 - (C_I^2/U^2) \tag{3.5}$$

$$D = \frac{C^2}{\omega_{p_-}^2} + \frac{p^{(0)+}B^2R_+^2}{8\pi\rho^2U^4(U^2-C_S^2)^2}\left\{U^4\left(\frac{7}{3}b_z^2 - b_x^2\right)(1+b_x^2)\right.$$

$$\left. + 4U^2C_S^2b_x^2[2b_x^2(1-2b_z^2) + \tfrac{1}{3}b_z^2] - C_S^4b_x^4(1-3b_x^2)^2\right\} \tag{3.6}$$

$$F = 1 + \frac{p^{(0)+}}{2\rho U^2(U^2-C_S^2)}\left[U^2(1+b_x^2) + b_x^2C_S^2(1-3b_x^2)\right] \tag{3.7}$$

$$G = \frac{C^2}{\omega_{p_-}^2} - \frac{p^{(0)+}B_x^2R_+^2}{8\pi\rho^2U^2(U^2-C_S^2)}\left\{U^2[1+3b_x^2(1+b_z^2)] - C_S^2b_x^2(1-3b_x^2)^2\right\} \tag{3.8}$$

$$r_m = \frac{C^2}{\omega_{p_-}^2}\frac{\nu}{U} \tag{3.9}$$

$p^{(0)+}$ is the zeroth order ion pressure and $R_+ = (p^{(0)+}/2\rho\Omega_+^2)^{1/2}$ is the ion gyro-radius based on the effective thermal speed $(p^{(0)+}/2\rho)^{1/2}$; $b_x = B_x/B$ and $b_z = B_z/B$ are the direction cosines of the magnetic field. Electron inertia dispersion, C/ω_{p_-}, has been retained for completeness. Equations (3.2) and (3.3) are to be solved subject to the boundary conditions that δB_z, $\delta B_y \to 0$ as $x \to \pm\infty$; i.e., the upstream and downstream states are uniform.

In their present form (3.2) and (3.3) are valid for both fast and slow shocks and could be analyzed directly. In order to focus on the wave trains for slow shocks, however, it is convenient to develop approximate forms of (3.2) and (3.3) in various limiting cases. The range of upstream slow shock flow velocities is given by the shock evolutionary conditions [12] as $C_I \geq U_1 > C_{SL}$. In addition, the restriction to magnetic slow shocks and the neglect of Debye length dispersion requires $U \ll C_S$. For $\beta \ll 1$, $C_{SL} \simeq C_S b_x$; hence $C_S \gg U > C_{SL}$ implies $b_x \ll 1$ or that low-β magnetic slow shocks propagate at large angles to the magnetic field. If $\beta \gg 1$ and $b_x \ll 1$, $C_{SL} \simeq C_I/(1 + 2/\beta)^{1/2}$; therefore the near equality of C_{SL} and C_I combined with $C_I \geq U > C_{SL}$ imply that high-β slow shocks are very weak. Note that for $\beta \gg 1$, $C_S \gg C_I$ so that $U \ll C_S$ is automatically satisfied. Recall that for exact parallel propagation, $C_I = C_{SL}$, and the slow shock is of zero strength.

The maximum strength slow shock occurs for $U_1 = C_I$ and has been termed the slow switch-off shock since the Rankine-Hugoniot relations require that the upstream magnetic field component in the shock plane be switched-off or reduced to zero across the shock [12]. Serious questions as to the hydromagnetic stability and existence of slow switch-off shocks have been raised by several authors [see Refs. 25-29]. In the present analysis, a premonition of difficulty with switch-off shocks is that for $U_1 = C_I$, $A_y = 0$. The vanishing of A_y in (3.3) requires that the inertial and ICR dispersion terms be balanced by the dissipative term, which is a worrisome conclusion since the collisionless shock wave train equations were derived in the limit of very weak dissipation. The problem of slow switch-off shocks will be discussed in Section 4.0 where it is shown from the full nonlinear differential equations in the low-β limit that dissipation is indeed crucial

for the steepening of the switch-off shock. The results obtained in this section will avoid the switch-off shock limit.

Proceeding now to approximate (3.2) and (3.3) for magnetic slow shocks, the discussion of Section 2.1 indicated that electron inertial dispersion does not contribute to the shock spatial structure, and hence C/ω_{p_-} can be neglected in D and G. For $\beta \ll 1$, $C/\omega_{p_+} \gg R_+$, and the ICR dispersion terms D and G can be neglected in the analysis of low-β oblique slow shocks. For $\beta \gg 1$ slow shocks, a convenient approximation is to expand D and G in the oblique shock limits $b_x \ll 1$ and the near parallel shock limit $b_z \ll 1$. With $U^2 \ll b_x^2 C_S^2$ the results are

a. $b_x \ll 1$

$$D = G = - \frac{p^{(0)+} C_I^2 b_x^2}{2\rho U^4} R_+^2 \equiv - E R_+^2 \tag{3.10}$$

b. $b_z \ll 1$

$$D = G = - \frac{2p^{(0)+} C_I^2}{\rho U^4} R_+^2 \equiv - E' R_+^2 \quad . \tag{3.11}$$

Similarly for $\beta \gg 1$, F can be approximated as

c. $b_x \ll 1$

$$F \simeq - \frac{p^{(0)+} b_x^2}{2\rho U^2} \tag{3.12}$$

d. $b_z \ll 1$

$$F \simeq - \frac{p^{(0)+} b_x^2}{\rho U^2} \quad . \tag{3.13}$$

The following analyses will be restricted to the limits $b_x << 1$ and $b_z << 1$.

3.3 Low-β Oblique Slow Shocks

After dropping electron inertial and ICR dispersion, (3.2) and (3.3) for the low-β oblique shock become

$$r_m \frac{d\delta B_z}{dx} - \frac{C}{\omega_{p_+}} \frac{C_I}{U} F \frac{d\delta B_y}{dx} = A_z \delta B_z \tag{3.14}$$

$$r_m \frac{d\delta B_y}{dx} + \frac{C}{\omega_{p_+}} \frac{C_I}{U} F \frac{d\delta B_z}{dx} = A_y \delta B_y \quad . \tag{3.15}$$

If δB_z and δB_y are taken to vary as $\exp(\lambda X)$, the solutions of the quadratic equation in λ obtained from (3.14) and (3.15) are

$$\lambda = \frac{\frac{1}{2}(A_y+A_z) r_m \pm \left[\frac{1}{4} r_m^2 (A_y-A_z)^2 - A_y A_z \frac{C^2}{\omega_{p_+}^2} \frac{C_I^2}{U^2} F^2 \right]^{1/2}}{\left[r_m^2 + \frac{C^2}{\omega_{p_+}^2} \frac{C_I^2}{U^2} F^2 \right]} \tag{3.16}$$

In the limit of weak resistive dissipation, $r_m << C/\omega_{p_+}$. If $A_y \neq 0$, i.e., the shock is far from the switch-off limit, (3.16) becomes approximately

$$\lambda \simeq \frac{(A_y+A_z)\, r_m}{2 \frac{C^2}{\omega_{p_+}^2} \frac{C_I^2}{U^2} F^2} \pm \frac{\sqrt{-A_y A_z}}{\frac{C}{\omega_{p_+}} \frac{C_I}{U} |F|} \tag{3.17}$$

a. Upstream Solution

About the upstream Rankine-Hugoniot conditions with $U^2 \ll C_S^2$, C_F^2 , $A_z \simeq (C_F^2/C_S^2)/[(M_{SL}^2-1)/M_{SL}^2]$, where $M_{SL} = U/C_{SL}$ is the slow shock Mach number. Since $U < C_I$ by the shock evolutionary conditions, $A_y < 0$; the positive root solution of (3.17) then yields an exponentially growing perturbation with increasing distance into the shock. Note that the negative root violates the upstream boundary condition δB_z, $\delta B_y \to 0$ as $X \to -\infty$. Therefore in the low-β oblique slow shock wave train the upstream magnetic field undergoes an exponential decrease with a characteristic scale length given by

$$L \sim \frac{|F| \dfrac{C_S}{C_F} \dfrac{C_I}{U} M_{SL}}{|\,[1-(C_I^2/U^2)](M_{SL}^2-1)\,|^{1/2}} \frac{C}{\omega_{p_+}} \quad . \tag{3.18}$$

All parameters in (3.18) are to be evaluated about the upstream flow conditions. For moderately strong slow shocks, $M_{SL}^2-1 \gg 1$, but still far from the switch-off limit, $C_I/U > 1$, the scale length (3.18) becomes $L \sim \sqrt{\beta_1}\,(C/\omega_{p_+}) \ll C/\omega_{p_+}$ if $\beta_1 \ll 1$; hence the leading edge can be sharper than C/ω_{p_+} .

b. Downstream Solution

Downstream both $A_z < 0$ and $A_y < 0$, (3.17) then describes a trailing oscillatory wave train with an oscillation length given by (3.18) evaluated about the downstream flow. As $x \to +\infty$ the wave train is exponentially damped to the uniform downstream state with a characteristic damping length $\sim [2(C^2/\omega_{p_+}^2)(C_I^2/U^2)F^2]/(A_y+A_z)r_m$. Note that A_y is always non-zero downstream, and therefore the above solution also applies to downstream switch-off shocks, if the term C_S/C_F in (3.18) is replaced by unity.

This solution is valid only if the downstream β is small. The obliquity restriction, $b_x << 1$, is somewhat relaxed, however, since the downstream flow speed is much less than the sound speed. Since the oblique slow shock converts magnetic energy into flow and thermal energy, even moderate strength slow shocks will produce a moderate to high-β downstream state, thus necessitating the consideration of ICR dispersion.

3.4 High-β ICR Slow Shocks

In the high-β limit the approximate equality of C_I and C_{SL} and the restriction of the upstream flow velocity to lie between $C_I > U > C_{SL}$ implies that the slow shock is weak, i.e., $M_{SL}^2 - 1 << 1$. Consequently the density jump across the shock is also small and the slow shock becomes almost incompressible [12]. Furthermore, most oblique slow shocks differ only slightly from complete switch-off shocks. Again the switch-off limit will be avoided in this section by taking $A_y \neq 0$ upstream, but will be discussed in Section 4.0.

For $\beta >> 1$, all terms in (3.2) and (3.3) contribute to the wave train structure. In order to simplify calculational details, only the very oblique, $b_x << 1$, and near parallel, $b_z << 1$, propagation limits will be considered so that the approximation expressions (3.10) - (3.13) for D, G, and F can be used. Again taking δB_z and δB_y to vary as $\exp(\lambda x)$, (3.2) and (3.3) reduce to the following fourth order algebraic equation for λ

$$\tilde{E}^2 R_+^4 \lambda^4 - 2r_m \tilde{E} R_+^2 \lambda^3 + \lambda^2 \left[\frac{C^2}{\omega_{p_+}^2} \frac{C_I^2}{U^2} F^2 + \tilde{E} R_+^2 (A_y + A_z) + r_m^2 \right]$$

$$- r_m (A_y + A_z)\lambda + A_y A_z = 0 \qquad (3.20)$$

$\tilde{E}$ takes on the value E if $b_x \ll 1$ and E' if $b_z \ll 1$. Noting that $C^2/\omega_{p_+}^2 = C_A^2/\Omega_+^2$, substituting (3.12) for F when $b_x \ll 1$, and (3.13) when $b_z \ll 1$, and using the definition of $\tilde{E}$ and A_y in the λ^2 term, (3.20) can be rewritten as

$$\tilde{E}^2 R_+^4 \lambda^4 - 2r_m \tilde{E} R_+^2 \lambda^3 + \lambda^2 [\tilde{E} R_+^2(1+A_z) + r_m^2]$$

$$- r_m \lambda(A_y+A_z) + A_y A_z = 0 \qquad (3.21)$$

To gain some insight into the solutions of (3.21), consider the dissipation less limit where $r_m = 0$. The solutions of the resulting quadratic in λ^2 are

$$\lambda^2 = \frac{1}{\tilde{E} R_+^2}\left[-\frac{(1+A_z)}{2} \pm \left(\frac{(1+A_z)^2}{4} - A_y A_z\right)^{1/2}\right] \qquad (3.22)$$

Since $A_z \approx (C_F^2/C_S^2)[(M_{SL}^2-1)/M_{SL}^2] \ll 1$ (note $C_F \approx C_S$ if $\beta \gg 1$), the square root in (3.22) can be expanded to obtain the following two approximate solutions

$$\lambda_+^2 \approx \frac{-A_y A_z}{\tilde{E} R_+^2(1+A_z)} \qquad (3.23)$$

$$\lambda_-^2 \approx -\frac{1+A_z}{\tilde{E} R_+^2} \qquad (3.24)$$

Upstream $A_y < 0$, $A_z > 0$ and (3.23) describes exponentially growing solutions; downstream $A_z < 0$, and the solutions are oscillatory. λ_-^2 is always negative, and hence yields oscillatory solutions both upstream and downstream.

Upon reexamination of (3.21) with $r_m = 0$, the λ_+^2 solution (3.23) is given by setting the last two terms equal to zero and the λ_-^2 solution

(3.24) arises by equating the first two terms to zero. Therefore, a reasonable approximation to the solutions of (3.21) with $r_m \neq 0$ is to take the last three terms and the first three terms separately equal to zero.

a. Solution of Last Three Terms

The solution for the quadratic in λ given by the last three terms of (3.21) is

$$\lambda_+ = \frac{\frac{r_m}{2}(A_y+A_z) \pm \left[\frac{1}{4} r_m^2 (A_y-A_z)^2 - A_y A_z \tilde{E} R_+^2 (1+A_z)\right]^{1/2}}{\tilde{E} R_+^2 (1+A_z) + r_m^2} \tag{3.25}$$

If $A_y \neq 0$ and $r_m \ll R_+$ in the weak dissipation limit, (3.25) can be approximated as

$$\lambda_+ \simeq \frac{r_m(A_y+A_z)}{2\tilde{E} R_+^2 (1+A_z)} \pm \frac{\sqrt{-A_y A_z}}{\sqrt{\tilde{E}(1+A_z)}\ R_+} \tag{3.26}$$

Since upstream $A_y < 0$, the positive root solution of (3.26), which satisfies the $x \to -\infty$ boundary condition, yields growing perturbations. Hence the upstream wave train structure is an exponential decrease of the magnetic field with a scale length

$$L \sim \left| \frac{\tilde{E}\left(1 + \frac{C_F^2}{C_S^2}\,\frac{M_{SL}^2-1}{M_{SL}^2}\right)}{\left(1 - \frac{C_I^2}{U^2}\right)\frac{C_F^2}{C_S^2}\,\frac{M_{SL}^2-1}{M_{SL}^2}} \right|^{1/2} R_+ \tag{3.27}$$

with all quantities evaluated about the upstream flow conditions. Since $M_{SL}^2 - 1 < 1$ and $|1 - C_I^2/U^2| < 1$ for $\beta \gg 1$, $L \gg R_+$, thus justifying the use of the small ICR expanded FCR-CGL fluid equations to describe the shock structure.

Downstream $A_y < 0$, $A_z < 0$, and the shock structure is a damped oscillatory trailing wave train with wave length given by (3.27) evaluated for downstream conditions. The exponential damping length is $\sim [2\tilde{E}R_+^2(1+A_z)]/[|A_y+A_z|r_m]$ and $A_y+A_z < 0$ assures satisfaction of the $x \to +\infty$ boundary conditions. Again note that the downstream solutions are also valid for slow switch-off shocks, provided that the terms C_F^2/C_S^2 in (3.27) are replaced by unity.

b. Solution of First Three Terms

Setting the first three terms of (3.21) to zero, the $r_m \neq 0$ solution corresponding (3.23) for $r_m = 0$ is

$$\lambda_- \approx \frac{r_m}{\tilde{E}\,R_+^2} \pm i\,\frac{\sqrt{1+A_z}}{\sqrt{\tilde{E}}\,R_+} \quad . \tag{3.28}$$

Although (3.28) yields damped oscillations as $x \to -\infty$, the oscillations grow exponentially as $x \to +\infty$, thus violating the downstream boundary conditions. Hence solution (3.28) must be rejected; the correct high-β slow shock wave train solution is, therefore, (3.25) or (3.26).

3.5 Summary

The structure of the slow shock nonlinear wave train differential equation has been examined by linearizing about the Rankine-Hugoniot stationary points. The low-β oblique slow shock wave train trails in the downstream flow and has an oscillation scale length of order C/ω_{p_+} . For $\beta >> 1$, the shock structure for both oblique and near-parallel propgation is also a trailing wave train with a scale length of order R_+ . Recall from Section 2.1 that both C/ω_{p_+} and R_+ dispersion decreased the linear slow wave

phase speed. Since wave trains are formed by waves on the same dispersion branch as the shock which phase stand in the shock flow, the downstream trailing nature of slow shock wave trains could have been anticipated from the linear dispersion relation. Although difficulty was encountered at the upstream point for slow switch-off shocks, the downstream trailing wave trains are valid even in the switch-off limit.

4.0 Slow Switch-Off Shocks

4.1 Introduction

Slow switch-off shocks, being the strongest slow shock, propagate at the maximum flow speed permitted by the shock evolutionary conditions, the intermediate wave speed ahead; the tangential magnetic field component is switched-off across the shock. An analogous shock flow occurs for parallel propagating low-β fast shocks. Here the Rankine-Hugoniot relations require a tangential component of the magnetic field to be switched-on across the shock; the downstream flow speed of fast switch-on shocks must equal the downstream intermediate wave speed [12].

Anderson [25] investigated the reflection and transmission of intermediate waves incident on plane fast and slow shocks using linear ideal or dissipationless hydromagnetic wave theory. He found that when the upstream slow shock and downstream fast shock flow velocities equaled the intermediate speed, the intermediate wave amplitude became infinite. Physically, because of the confluence of the intermediate wave and shock flow speeds, intermediate waves are resonately generated and accumulate in the shock front. Anderson concluded from the breakdown of the small disturbance linear theory that the slow switch-off and fast switch-on shock fronts are unstable and would disintegrate. Slow (fast) shocks which are slightly weaker than switch-off (switch-on) shocks, however, are stable.

An alternative argument for the existence of stable switch-on and switch-off shocks has been advanced by Kantrowitz and Petschek [12]. They consider the well-posed shock piston problem in which the driving piston moving parallel to a strong magnetic field (low-β) is accelerated to a speed less than the intermediate wave speed. For parallel shocks such a downstream flow speed

could be obtained from the gas dynamic Rankine-Hugoniot relations in which the parallel magnetic field does not enter. In the hydromagnetic shock theory, however, this flow corresponds to an extraneous and thus disallowed shock solution. Kantrowitz and Petschek argue that the resolution of this piston problem is that a fast switch-on shock first reduces the flow velocity to the intermediate speed and then is immediately followed by a slow switch-off shock which further reduces the flow speed below the intermediate speed and annihilates the switched-on tangential magnetic field component. Here the two shocks simply propagate together. Furthermore, if the boundary conditions at the piston also require a rotation of the magnetic field and the annihilation of the tangential component, Kantrowitz and Petschek, and Petschek and Thorne [30], have argued that the rotation is first accomplished by the intermediate wave without change of field magnitude, and then the slow switch-off shock reduces the field magnetic without further rotation. Here the intermediate wave and slow switch-off shock simply propagate together.

Chu and Taussig [28] numerically investigated fast switch-on shocks using the nonlinear hydromagnetic equations with an effective numerical dissipation. After the switch-on shock was launched by a piston, the shock encountered an upstream transverse magnetic perturbation. The shock structure repolarized in order to adjust to the new magnetic field orientation, and an intermediate wave was produced downstream which then rotated the magnetic field so that the piston magnetic boundary conditions were satisfied. For the slow switch-off shock the intermediate wave rotates the magnetic field ahead of the shock so that the piston boundary conditions are satisfied. Chu and Taussig concluded that fast switch-on and slow switch-off shocks were stable to intermediate wave perturbations.

The significance of the Kantrowitz and Petschek existence arguments and the analysis of Chu and Taussig is that they are based on the causality of the piston problem, and hence include not only the nonlinear shock and intermediate wave properties but also dissipation. Anderson's [25] non-existence argument, on the other hand, was based on linear, dissipationless hydromagnetic theory; thus an infinite amplitude resonance, a not surprising phenomenon in dissipationless theory, was found. Recall from Section 3.2 that in the switch-off shock limit $A_y = 0$, the dispersion terms in the linearized wave train differential equation (3.3) had to be balanced by the resistive dissipation term. This conclusion and the Kantrowitz and Petschek existence arguments suggest that the structure of switch-off and switch-on shocks depends critically on the presence of dissipation.

In Section 4.2 the full nonlinear dissipative wave train differential equations for a low-β oblique slow switch-off shock is derived. For simplicity, only ion inertial dispersion is included. The analysis of these equations reveals the importance of dissipation in the shock structure. In Section 4.3 the linearized wave train analysis of Section 3.0 is re-examined in the switch-off limit for both low and high-β slow shocks. Section 4.4 presents a further discussion of the switch-off shock problem.

4.2 Low-β Oblique Slow Switch-off Shock Wave Train

The derivation of the switch-off shock wave train differential equation commences from the nonlinear system of equations (2.5) - (2.11). For $\beta << 1$ the ICR dispersion terms can be dropped; again assuming pressure isotropy then yields $P_{xx}^{(1)} = P$, $P_{xy}^{(1)} = 0$, $P_{xz}^{(1)} = 0$, and $(\underset{\sim}{q}_{\perp}^{(1)} + \underset{\sim}{q}_{\parallel}^{(1)}) \cdot \hat{x} = 0$. As before, zero order parallel heat flow will be neglected. In addition only ion inertial dispersion is retained in Ohm's Law (2.10) and (2.11). The

calculation proceeds as in Section 3.0 for the linearized differential equations. In (2.6) - (2.9), P, V_y, and V_z are eliminated, and U is determined in terms of B_z and B_y. Then U, V_y, and V_z are eliminated from Ohm's Law (2.10) and (2.11) to yield the following two differential equations

$$r_m' \frac{dB_z}{d\tau} - \frac{\cot\phi}{M_A} \frac{dB_y}{d\tau} = (B_z-1)\left(1 - \frac{\cot^2\phi}{M_A^2}\right) + B_z f(B_z, B_y) \tag{4.1}$$

$$r_m' \frac{dB_y}{d\tau} + \frac{\cot\phi}{M_A} \frac{dB_z}{d\tau} = B_y\left(1 - \frac{\cot^2\phi}{M_A^2}\right) + B_y f(B_z, B_y) \tag{4.2}$$

where

$$f(B_z,B_y) = \frac{1}{\gamma+1}\left\{\frac{M_S^2-1}{M_S^2} - \frac{\gamma(B_z^2+B_y^2-1)}{2M_A^2} - \left[\left(\frac{M_S^2-1}{M_S^2} - \frac{\gamma(B_z^2+B_y^2-1)}{2M_A^2}\right)^2 - (\gamma^2-1)\frac{B_y^2 + (B_z-1)^2}{M_A^2}\left(1 - \frac{\cot^2\phi}{M_A^2}\right) - (\gamma+1)\frac{B_y^2 + B_z^2 - 1}{M_A^2}\right]^{1/2}\right\} \tag{4.3}$$

In (4.1) - (4.3), B_z and B_y have been normalized to B_{z_1}. $B_{y_1} = 0$ was assumed, although there would be no change in following analysis and conclusions if $B_{y_1} \neq 0$. $M_A = [U_1(4\pi\rho_1)^{1/2}]/B_{z_1}$ is the upstream Alfven Mach number and $M_S = U_1/(\gamma P_1/\rho_1)^{1/2}$ is the corresponding sonic Mach number; the ratio of specific heats $\gamma = 5/3$. $\cot\phi = B_x/B_{z_1}$. $r_m' = (\nu/\Omega_-)(1/M_A)$ where $\Omega_- = eB/M_-c$. The pseudo-time variable $d\tau = dx U_1 \omega_{p_+}/U(x)c$ where $\omega_{p_+} = (4\pi N_1 e^2/M_+)^{1/2}$. Note that the right-hand-sides (RHS) of (4.1) and (4.2)

are independent of derivatives and contain only hydromagnetic quantities. Setting the RHS to zero, i.e., spatially uniform conditions, yields the Rankine-Hugoniot relations for B_z and B_y.

For the slow switch-off shock, $U_1 = C_{I_1} = B_x/(4\pi\rho_1)^{1/2}$ or $M_A = \cot\phi$. Therefore in the switch-off limit (4.1) and (4.2) simplify to

$$r_m' \dot{B}_z - \dot{B}_y = f(r)\, B_z \tag{4.4}$$

$$r_m' \dot{B}_y + \dot{B}_z = f(r)\, B_y \tag{4.5}$$

where dot $(\cdot)$ denotes $d/d\tau$. From (4.3) f is now a function only of $r = (B_z^2 + B_y^2)^{1/2}$; note that $f(r=1) = 0$ so that $f(r)$ vanishes at upstream Rankine-Hugoniot conditions. The RHS of (4.4) and (4.5) can be interpreted as a pseduo-force which yields a stationary point of the differential equations at $r = 1$. The stability of the corresponding pseudo-potential about $r = 1$ is determined by taking the appropriate derivatives of the RHS of (4.4) and (4.5) and evaluating them at $B_{y_1} = 0$ and $B_{z_1} = 1$ to obtain

$$\frac{\partial}{\partial B_z}\left[f(r)B_z\right]_{B_z=1,B_y=0} = \frac{1}{4\pi\rho_1}\,\frac{1}{C_{S_1}^2 - U_1^2} \equiv \Delta \tag{4.6}$$

$$\frac{\partial}{\partial B_y}\left[f(r)B_y\right]_{B_z=1,B_y=0} = 0 \quad . \tag{4.7}$$

Since $U_1 \ll C_{S_1}$ for oblique magnetic slow shocks, (4.6) implies that at the upstream point $r = 1$ the pseudo-potential has an unstable maximum with-respect-to (wrt) B_z and is neutrally stable wrt B_y. Hence $r = 1$ is a saddle or inflection point of the pseudo-potential. Furthermore since the

pseudo-potential is obtained in the usual way by integrating (4.4) wrt B_z and (4.5) wrt B_y, equating and normalizing, the pseudo-potential is only a function of r, and hence is symmetric in B_z and B_y.

Equations (4.4) and (4.5) can be expressed in an alternate and more transparent form. Multiplication of (4.4) by B_y and (4.5) by B_z and then subtraction of the results yield

$$B_y\dot{B}_y + B_z\dot{B}_z + r_m'(\dot{B}_yB_z - \dot{B}_zB_y) = 0 \tag{4.8}$$

If the cylindrical coordinates $B_z = r\cos\theta$ and $B_y = r\sin\theta$ are introduced, (4.8) becomes

$$\dot{r}/r = -r_m'\,\dot{\theta} \quad . \tag{4.9}$$

With the upstream $\tau \to -\infty$ boundary conditions $r = 1$, $\theta = 0$, (4.9) can be immediately integrated to obtain

$$r(\tau) = \exp[-r_m'\,\theta(\tau)] \quad . \tag{4.10}$$

Similarly, multiplying (4.4) by $\dot{B}_y$ and (4.5) by $\dot{B}_z$ and subtracting yields

$$\dot{r}^2/r^2 + \dot{\theta}^2 = -f(r)\,\dot{\theta} \quad . \tag{4.11}$$

After elimination of $\dot{\theta}$ in (4.11) by substitution from (4.9), (4.11) reduces to

$$\frac{\dot{r}}{r}\left[\frac{\dot{r}}{r}\left(1 + \frac{1}{r_m'^2}\right) - \frac{f(r)}{r_m'}\right] = 0 \quad . \tag{4.12}$$

Thus the slow switch-off wave train differential equation factors into two solutions.

First consider the $\dot{r} = 0$ solution in which the magnetic field magnitude

is constant. If $r_m' \neq 0$, $\dot{r} = 0$ in (4.9) requires $\dot{\theta} = 0$, and the magnetic field direction is unchaged. If there is no dissipation $r_m' = 0$, from (4.11) the $\dot{r} = 0$ solution yields $\dot{\theta} = -f(r_o)$ which can be integrated to obtain

$$\theta(\tau) = - f(r_o)\, \tau \quad . \tag{4.13}$$

If $r_o \neq 1$ so that $f(r_o) \neq 0$ and the flow does not satisfy the upstream Rankine-Hugoniot relations, (4.13) describes the rotation of a constant amplitude magnetic field, and therefore represents the intermediate wave. At the upstream point $r_o = 1$, (4.13) yields $\theta(\tau) = 0$, and no rotation of the magnetic field occurs. In conclusion, the $\dot{r} = 0$ solution does not permit a dissipative intermediate wave, which would change the plasma state, and if the upstream flow satisfies the Rankine-Hugoniot relations, no intermediate wave is required. If the boundary conditions of a piston problem involving a switch-off shock did require an upstream intermediate wave, however, the upstream flow would not be in the Rankine-Hugoniot configuration given by $f(r)$ until after the passage of the intermediate wave. Hence, in concurrence with the results of Kantrowitz and Petschek [12] and of Chu and Taussig [28] an intermediate wave and switch-off shock could exist together with each satisying separate boundary conditions.

Now consider the second solution of (4.12). In the dissipationless limit $r_m' = 0$, the second solution requires that $\dot{r} = 0$ and $f(r) = 0$ or $r = 1$; without dissipation no transition from the upstream state occurs. For $r_m' \neq 0$, (4.12) yields the immediate quadrature

$$\frac{\tau}{r_m' \left(1 + \dfrac{1}{r_m'^2} \right)} = \int \frac{dr}{f(r)\, r} \tag{4.14}$$

The nature of this solution can be examined by linearizing about the upstream point $r = 1$. For $r = 1 + \delta r$, $\theta = \delta\theta$, and $f(1+\delta r) = \Delta\delta r$ where $\Delta > 0$ is given by (4.6), the linearized solution of (4.14) becomes

$$\delta r \propto \exp\left[\frac{\Delta\tau}{r_m'\left(1 + \frac{1}{r_m'^2}\right)}\right] \quad . \tag{4.15}$$

From (4.9) $\delta\theta$ is given by

$$\delta\theta \propto \frac{-1}{r_m'}\ \delta r \quad . \tag{4.16}$$

Hence $\delta r \to 0$ and $\delta\theta \to 0$ as $\tau \to -\infty$, thus satisfying the upstream boundary conditions. As τ increases positively toward downstream, δr and therefore r leave the upstream state exponentially, and the magnetic field direction begins to rotate. Since the second solution yields a transition from the upstream Rankine-Hugoniot state, (4.14) represents the slow switch-off shock. Therefore the switch-off shock transition from the upstream state occurs only in the presence of dissipation.

In the weak dissipation limit $r_m' \ll 1$, from (4.15) and (4.16) the magnitude of the upstream magnetic field changes slowly compared to the change in field direction. Therefore since $f(r)$ will be slowly varying, an approximate or adiabatic solution for $\theta(\tau)$ can be obtained by substituting (4.9) into (4.11) and integrating the result with $f(r)$ held constant to obtain

$$\theta(\tau) \simeq -\frac{f(r)}{1 + r_m'^2}\ \tau \quad . \tag{4.17}$$

Recall that $d\tau = dx U_1 \omega_{p_+}/CU(x)$; it can easily be shown from (2.6) - (2.9) that

$$\frac{U(x)}{U_1} = 1 + f(r) \quad . \tag{4.18}$$

Hence with $f(r)$ slowly varying, (4.17) becomes

$$\theta(x) = \frac{-f(r)\, x}{\frac{c}{\omega_{p_+}} [1+f(r)] \left[1 + \frac{r_m^2}{c^2/\omega_{p_+}^2} \right]} \tag{4.19}$$

From (4.10) and (4.19) an approximate solution for the upstream magnetic field then becomes

$$B_z(x) = \exp \left[\frac{-r_m\, \theta(x)}{c/\omega_{p_+}} \right] \cos \theta(x)$$

$$B_y(x) = \exp \left[\frac{-r_m\, \theta(x)}{c/\omega_{p_+}} \right] \sin \theta(x) \tag{4.20}$$

Note that for $r < 1$, $f(r) < 0$ and $\theta(x) > 0$; hence from (4.18) $U(x) < U_1$ and from (4.20) $B_z(x)$ and $B_y(x)$ decrease in magnitude as x increases.

The spatial structure of collisionless slow switch-off shocks is now apparent. The magnetic field magnitude inside the shock gradually decreases from the upstream value with an exponential scale length $L \sim c^2/\omega_{p_+}^2\, r_m >> c/\omega_{p_+}$. The magnetic field direction rotates rapidly with an oscillation wavelength $\sim c/\omega_{p_+}$. Since $f(r)$ varies on the $c^2/\omega_{p_+}^2\, r_m$ scale length, the flow velocity from (4.18) and hence the density decrease gradually so that the shock leading edge is nearly incompressible. From Section 3.0 the downstream wave train structure is also a rotating magnetic field with wavelength c/ω_{p_+} or R_+ which slowly damps to $B_y = B_z = 0$. The complete switch-off shock structure will then consist of a long trailing wave train

of magnetic field rotations which are gradually damped by resistivity to a uniform downstream state. A sketch of the wave train is given in Figure 2.

The above discussion can easily be reformulated for the fast switch-on shock. If all plasma parameters are normalized to the downstream flow conditions, (4.4) and (4.5) are recovered, and the analysis proceeds as for the slow switch-off shock. Therefore the fast switch-on shock structure is a long train of magnetic rotations starting from $B_y = B_z = 0$. The magnetic field magnitude gradually increases through the shock until the downstream state is reached. A sketch of the fast switch-on shock wave train can be obtained from Figure 2 by interchanging the upstream and downstream states for the magnetic field. A similar spatial structure for the fast switch-on shock has been observed in shock experiments at Novosibirsk (R. Z. Sagdeev, private communication).

4.3 Switch-off Shocks from the Linearized Wave Train Equations

The previous section established that dissipation determines the leading edge switch-off shock wave train structure. Returning to the linearized analysis of Section 3.0, the switch-off limit $A_y = 0$ can now be taken with confidence. About the upstream point of low-β oblique slow shocks, (3.16) with $A_y = 0$ yields one root $\lambda = 0$ which corresponds to the $\dot{r} = 0$ solution, and the second root which describes the exponential decrease of the magnetic field with scale length

$$L \sim \frac{\left[r_m^2 + \frac{c^2}{\omega_{p_+}^2} F^2 \right]}{\frac{C_F^2}{C_S^2} \frac{M_{SL}^2 - 1}{M_{SL}^2} r_m} \qquad (4.21)$$

(4.21) corresponds to the solutions (4.15) and (4.16).

The range of flow velocities for which (4.21) rather than (3.18) applies can be roughly estimated by equating the two terms under the radical in (3.16). Noting that for $\beta \ll 1$, $M_{SL}^2 - 1 \simeq M_{SL}^2$ if $U \sim C_I$, and $\beta \sim C_S^2/C_F^2$, the two terms are comparable when $|U^2 - C_I^2|/U^2 \approx (1/4\beta)(\nu^2/\Omega_-^2)(B^2/B_x^2)$. Hence if $\nu/\Omega_- \ll 1$ and β and B_x/B are only moderately small, the flow velocity must nearly equal the intermediate speed in order for the switch-off shock solution to apply.

For high-β switch-off shocks the solution (3.25) with $A_y = 0$ describes the ICR dispersive structure. One solution of (3.25) is $\lambda = 0$; the second solution yields the upstream magnetic field decreasing exponentially with a scale height

$$L \sim \frac{\tilde{E} R_+^2 \left(1 + \frac{C_F^2}{C_S^2} \frac{M_{SL}^2 - 1}{M_{SL}^2} \right) + r_m^2}{\frac{C_F^2}{C_S^2} \frac{M_{SL}^2 - 1}{M_{SL}^2} r_m} \qquad (4.22)$$

Since for $\beta \gg 1$ all but the very weakest slow shocks are near the switch-off limit, (4.22) should describe the leading edge structure of most high-β slow shocks. Since $r_m \ll R_+$ for weak dissipation, (4.18) predicts a very thick $L \gg R_+$ leading edge structure. Note that the solution (3.28) is unchanged when $A_y = 0$ and is still disallowed by the boundary conditions.

4.4 Wave Train Structure of Slow Shocks

Upon comparing the results of Sections 3.0 and 4.0, the thickness of the slow shock leading edge exhibits a curious behavior with increasing shock strength. As the Mach number increases, (3.18) for $\beta \ll 1$ and (3.27) for $\beta \gg 1$, predicts that the shock thickness initially decreases. However, as the switch-off limit is approached, the $1/|1 - C_I^2/U^2|^{1/2}$ term in (3.18) or

(3.27) causes the shock thickness to increase until the limiting scale length set by resistivity, (4.21) or (4.22) is reached (see Figure 3). (If the shock is strongly dissipative, $r_m > c/\omega_{p_+}$ or R_+, and the shock thickness is always given by r_m.)

In order to understand the increase of shock thickness with Mach number and the resistive structure of switch-off shocks, consider the steepening of a pulse emitted by a piston which has been accelerated to the downstream flow conditions of a switch-off shock. Pulse steepening proceeds by the nonlinear excitation of waves with frequencies and wave numbers at harmonic multiples of the fundamental wave from which the pulse started. As steepening continues, the plasma conditions inside the pulse approach the downstream shock conditions; hence the fluid velocity inside the pulse is less than the phase speed of the emitted harmonic waves. These waves then propagate upstream against the fluid flow toward the pulse front and pile up, thus resulting in further steepening and acceleration of the pulse.

In a collision dominated plasma, steepening limitation arises when the wavelengths of the emitted harmonic waves become comparable to dissipation scale lengths such as r_m. Dissipation slows the phase speed of the emitted waves to below the fluid velocity inside pulse so that all waves are blown downstream by the fluid and steepening ceases. In a collisionless plasma, dispersion at short wavelengths reduces the wave phase speed below the fluid velocity and thus limits pulse steepening.

Now consider the plasma state inside the pulse which is steepening into a magnetic switch-off shock. The downstream β_2 for the switch-off shock obtained from the Rankine-Hugoniot relations is given by

$$\beta_2 = \frac{8\pi P_2}{B_x^2} = \frac{2\gamma+1}{\gamma+1}\frac{8\pi P_1}{B_x^2} + \frac{1}{\gamma+1}\left(\frac{B_{z_1}^2}{B_x^2} - 2\right)$$

$$+ \frac{2}{\gamma+1}\left[\left(1 - \frac{4\pi\gamma P_1}{B_x^2} + \frac{\gamma B_{z_1}^2}{B_x^2}\right)^2 + \frac{(\gamma+1)B_{z_1}^2}{B_x^2}\right]^{1/2} \qquad (4.23)$$

Since for low-β magnetic slow shocks $B_z/B_x \gg 1$, β_2 is always exceeds unity. Hence as the pulse speed approaches the upstream intermediate speed, inside the pulse β becomes greater than unity. Furthermore the magnetic field in the pulse center approaches $B_y = B_z = 0$.

The slow harmonic waves emitted by the steepening process, therefore, propagate almost parallel to the local magnetic field inside the pulse and, since $\beta > 1$, their phase velocity is almost the intermediate speed. Hence the harmonic slow waves are almost completely rotational and nearly incompressible. Although still propgating faster than the local fluid velocity, the incompressible rotational harmonic waves cannot contribute to shock steepening. In addition, as demonstrated in Section 4.2, for flow velocities near the intermediate speed, ion inertia only produces rotations of the magnetic field so that dispersion cannot limit shock steepening. Therefore steepening up to the intermediate speed ahead and steepening limitation can only be accomplished by dissipation. The switch-off shock steepening length or the thickness of the leading edge increases until it is finally stopped by resistivity. Hence the leading edge structure is controlled by magnetic resistive diffusion with dispersion producing only rotations of the magnetic field direction.

5.0 Discussion

5.1 Summary of Magnetic Slow Shock Results

The wave train structure of magnetic slow shocks, i.e., slow shocks whose upstream flow velocity is much less than the sound speed, was investigated using the fluid equations of FCR-CGL hydromagnetics. These fluid equations contain two difficulties which limit their applicability to shock studies. A sufficient number of conservation relations does not exist to uniquely determine the downstream state independent of the shock dissipation. In order to pursue a fluid analysis of slow shocks without first solving for the collisionless turbulent dissipation, the pressure anisotropy was assumed to be of lower order in the expansion parameter (R_+/L) then the ICR dispersion terms, thus providing a closed set of conservation relations. An additional difficulty inherent in fluid moment hierarchies is that the third order moment or zeroth order parallel heat flow is not determined by the fluid equations, but depends on the form of the kinetic distribution functions and the collisionless turbulence. To truncate the hierarchy, heat flow and higher order moments were assumed to be of order $(R_+/L)^3$, and hence could be neglected in comparison with ICR dispersion.

The slow shock wave train differential equations were examined by linearizing about the asymptotic Rankine-Hugoniot stationary points, thus enabling determination of the shock structure at the leading and trailing edges. Low-β switch-off shocks were studied from the nonlinear wave train equations. The results are:

a. Low-β Oblique Slow Shock

For shock strengths weaker than the switch-off limit, the upstream magnetic field decreases exponentially with the thickness scaling as c/ω_{p_+}

A weakly damped wave train trails in the downstream flow with oscillation wavelengths of order c/ω_{p_+} provided $\beta < 1$ downstream. For low-β oblique shocks of moderate strength, the large magnetic energy dissipation is likely to produce a $\beta > 1$ downstream flow, so that the trailing wave train should have R_+ oscillation lengths. Hence these shocks should possess multiply dispersive wave train structure.

b. High-β Slow Shocks

For very weak oblique and near-parallel $\beta >> 1$ slow shocks, the wave train trails in the downstream flow with wavelengths of order R_+ .

c. Slow Switch-off Shocks

In the leading edge of switch-off shocks the magnetic field magnitude resistively diffuses from the upstream state with a scale length $L \sim c^2/\omega_{p_+}^2 r_m$ or R_+^2/r_m . Without dissipation no shock transition occurs, and only intermediate wave solutions are allowed provided the flow does not satisfy the Rankine-Hugoniot relations. The switch-off shock spatial structure is a long train of rotational oscillations which start upstream and are gradually resistively damped to a uniform downstream state. The oscillation scale length will locally be c/ω_{p_+} if $\beta < 1$ or R_+ if $\beta > 1$.

In previous collisionless shock investigations the dissipationless wave train differential equations describe a symmetrical solitary wave across which the plasma state remains unchanged [1]. In the pseudo-potential analogy, the solitary wave corresponds to a particle which leaves the upstream unstable maximum and executes one oscillation in the pseudo-potential well before returning to the original state. These shock-like solitons are formed by balancing pulse steepening against dispersive wave propagation, and with the addition of dissipation are converted into shock wave trains. Since the switch-off shock wave train differential equations without dissipation admit

no solutions which leave the upstream state, there is no solitary wave corresponding to the switch-off shock. In the switch-off limit, dispersion alone cannot balance shock steepening to form a soliton, and the only permitted steady state flow requires magnetic resistive diffusion to limit steepening.

d. Fast Switch-on Shocks

The wave train equations for the low-β parallel fast switch-on shock are formally identical to those for the oblique low-β switch-off shock. Therefore the switch-on shock structure is a long train of c/ω_{p_+} wavelength magnetic rotations with slowly growing amplitude. Resistivity is required to reduce the downstream flow speed to the intermediate speed.

5.2 High-β Oblique Fast Shocks

The linearized wave train differential equations (3.2) and (3.3) contain both fast and slow shocks. Since low-β fast shocks have been examined by various authors (see Refs. 1, 2), only $\beta >> 1$ fast shocks will be mentioned here. Furthermore, since the parallel high-β fast shock is primarily electrostatic, only very oblique magnetic fast shocks will be considered. The analysis proceeds exactly as for slow shocks. At the leading edge of the fast shock wave train, the magnetic field undergoes an exponential rise with scale length

$$L \sim \left[\frac{7\, p^{(0)+}\, B_z^{\,2}}{24\pi\, \rho^2 C_F^{\,2} (U^2 - C_S^{\,2})} \right]^{1/2} \frac{R_+}{(M_F^{\,2}-1)^{1/2}} \tag{5.1}$$

Downstream the wave train trails with an oscillation length given in (5.1) evaluated about the downstream flow. A trailing ICR wave train for perpendicular fast shocks has been derived by Kinsinger and Auer [31].

The above solution is valid for a very small parameter range, however. In particular, for resistivity alone to provide the shock dissipation, the downstream flow speed must exceed the sound speed, thus restricting the solution to very weak shocks. Viscous dissipation or an ion acoustic subshock [24] is needed to go below the sound speed. In addition for the perpendicular ICR fast shock, the scale length in (5.1) becomes less than R_+ for Mach numbers less than about two; Coroniti [32] has shown that for stronger fast shocks ICR dispersion no longer contributes to the wave train structure, and the perpendicular shock structure becomes an electron inertial length trailing wave train. For strong oblique fast shocks, a leading c/ω_{p_+} length wave train could occur.

5.3 Heat Flow and Magnetic Slow Shocks

The most uncertain aspect of the slow shock wave train analysis is the neglect of heat flow along the magnetic field. Although resistivity alone provides sufficient dissipation for magnetic slow shocks [13], thermal conduction dissipation could modify the shock structure. For example, assume that an anomalous heat conduction term is included in the energy equation and that the thermal conduction scale length is much longer than the resistive diffusion length. Heat conduction would then form a thick leading edge to the shock. The flow velocity is gradually reduced until it locally equals the linear slow wave speed defined as in (2.2) except that the sound speed is replaced by the isothermal or $\gamma = 1$ sound speed, P/ρ. At this point in the shock an isothermal discontinuity occurs which decouples the temperature and density so that downstream of the discontinuity the flow is isothermal. The additional dissipation required to further reduce the flow velocity to the downstream Rankine-Hugoniot value is accomplished by a resistive subshock.

In a collisionless slow shock heat conduction need not be restricted to anomalous thermal conduction. Oblique low-β and all high-β slow shocks have flow speeds which are small compared to the downstream ion thermal speed. Therefore the containment of hot ions behind the shock presents a formidable difficulty; electrons, because of their small inertia, can usually be dragged through the shock by a small electric field. In low-β near switch-off shocks, hot ions flowing back upstream would encounter a strong mirror field and be reflected. Some hot ions, however, would always be in the loss cone and would penetrate upstream; the loss cone flux might be maintained by downstream ion pitch-angle scattering. In high-β slow shocks, mirror field containment would be relatively ineffective. Hence in collisionless slow shocks the suppression of hot ion heat flow upstream probably requires an ion heat flow instability analogous to the electron heat flow instabilities analyzed by Forslund [33] for the solar wind.

APPENDIX

A.1 Pressure Tensor $\underset{\approx}{P}^{(1)}$ and ICR Heat Flow $\underline{q}_{\perp}^{(1)} + \underline{q}_{\perp}^{(1)}$

In deriving the FCR-CGL equations, MacMahon [14] employed a coordinate system oriented about the magnetic field direction. The basis vectors are $\hat{e}_3 = \hat{B}$, $\hat{e}_1$ is in the direction of the principal normal, and $\hat{e}_2 = \hat{e}_3 \times \hat{e}_1$. After assuming pressure isotropy through first order, and neglecting the zeroth order parallel heat flow and higher order moments, the first order pressure tensor $\underset{\approx}{P}^{(1)}$ becomes the sum of the following tensors

$$(\underset{\approx}{P}^{(1)} : \underset{\approx}{I})\ \underset{\approx}{I} = P^{(1)}\underset{\approx}{I} \tag{A.1.1}$$

$$\underset{\approx\delta}{P}^{(1)} = -\frac{P^{(0)+}}{2\Omega_+}\underset{\approx\gamma}{I} : [\nabla\underline{V}^+]\ \underset{\approx\delta}{I} \tag{A.1.2}$$

$$\underset{\approx\gamma}{P}^{(1)} = \frac{P^{(0)+}}{2\Omega_+}\underset{\approx\delta}{I} : [\nabla\underline{V}^+]\ \underset{\approx\gamma}{I} \tag{A.1.3}$$

$$\underset{\approx 13}{P}^{(1)} + \underset{\approx 31}{P}^{(1)} = \hat{e}_1 \cdot \left[\frac{P^{(0)+}}{\Omega_+}\hat{e}_3 \times (\hat{e}_3\cdot\nabla\underline{V}^+ + (\nabla V^+)\cdot\hat{e}_3)\right](\hat{e}_2\hat{e}_3 + \hat{e}_3\hat{e}_2) \tag{A.1.4}$$

$$\underset{\approx 23}{P}^{(1)} + \underset{\approx 32}{P}^{(1)} = \hat{e}_2 \cdot \left[\frac{P^{(0)+}}{\Omega_+}\hat{e}_3 \times (\hat{e}_3\cdot\nabla\underline{V}^+ + (\nabla\underline{V}^+)\cdot\hat{e}_3)\right](\hat{e}_2\hat{e}_3 + \hat{e}_3\hat{e}_2) \tag{A.1.5}$$

where $\underset{\approx\delta}{I} = \hat{e}_1\hat{e}_1 - \hat{e}_2\hat{e}_2$, $\underset{\approx\gamma}{I} = \hat{e}_1\hat{e}_2 + \hat{e}_2\hat{e}_1$, and $\underset{\approx}{I}$ is the unit tensor. $P^{(0)+}$ is the zeroth order ion pressure, and $P^{(1)}$ is the first order pressure. $\underline{V}^+$ is the ion velocity which, to lowest order, is just the fluid velocity $\underline{V}$.

The first order ICR perpendicular heat flows are

$$\underset{\sim}{q}_{\perp}^{(1)} = \frac{2P^{(0)+}}{\Omega_+ \rho} \hat{e}_3 \times (\nabla \cdot \underset{\approx}{P}^{(1)}) \tag{A.1.6}$$

$$\underset{\sim}{q}_{\perp}^{\prime\prime(1)} = \frac{P^{(0)+}}{2\Omega_+ \rho} \hat{e}_3 \times (\nabla \cdot \underset{\approx}{P}^{(1)}) \tag{A.1.7}$$

Note that although $\underset{\sim}{q}_{\perp}^{(1)}$ and $\underset{\sim}{q}_{\perp}^{\prime\prime(1)}$ are formally first order in (R_+/L), $\nabla \cdot \underset{\approx}{P}^{(1)}$ enters in (A.1.6) and (A.1.7) rather than $\nabla \cdot \underset{\approx}{P}^{(0)}$. It is easily shown that $\hat{e}_3 \times \nabla \cdot \underset{\approx}{P}^{(0)} = 0$. $\nabla \cdot \underset{\approx}{P}^{(1)}$ is retained since in the energy equation (2.9) the ICR terms enter to the order $(R_+/L)^2$. MacMahon [34] has shown that the ICR contributions from $\nabla \cdot \underset{\approx}{P}^{(1)}$ in $\underset{\sim}{q}_{\perp}^{(1)}$ and $\underset{\sim}{q}_{\perp}^{\prime\prime(1)}$ actually provide the dominant ICR dispersion for the linear perpendicular fast wave and for perpendicular fast shocks.

Planar shocks, however, are basically Cartesian so that it is necessary to transform (A.1.1) - (A.1.7) into the Cartesian basis x, y, z. From (2.6) - (2.9) only the components $P_{xx}^{(1)}$, $P_{xy}^{(1)}$, $P_{xz}^{(1)}$, and $(\underset{\sim}{q}_{\perp}^{(1)} + \underset{\sim}{q}_{\perp}^{\prime\prime(1)}) \cdot \hat{x}$ are needed. Skipping the trivial coordinate transformation, the needed components are

A. $$P_{xx}^{(1)} = P^{(1)} + T_{xx} \tag{A.1.8}$$

$$T_{xx} = T_{xx}^{y} \frac{dV_y}{dx} + T_{xx}^{z} \frac{dV_z}{dx} \tag{A.1.9}$$

$$T_{xx}^{y} = -\frac{P^{(0)+}}{2\Omega_+} b_z (1 + 3 b_x^2) \tag{A.1.10}$$

$$T_{xx}^{z} = \frac{P^{(0)+}}{2\Omega_+} b_y (1 + 3 b_x^2) \tag{A.1.11}$$

B. $$P_{xy}^{(1)} = T_{xy}^{x} \frac{dU}{dx} + T_{xy}^{z} \frac{dV_z}{dx} \tag{A.1.12}$$

$$T^x_{xy} = - T^y_{xx} \tag{A.1.13}$$

$$T^z_{xy} = \frac{p^{(0)+}}{2\Omega_+} b_x (1 - 3 b_x^2) \tag{A.1.14}$$

C. $$p^{(1)}_{xy} = T^x_{xz} \frac{dU}{dx} + T^y_{xz} \frac{dV_y}{dx} \tag{A.1.15}$$

$$T^x_{xz} = - \frac{5}{2} \frac{p^{(0)+}}{\Omega_+} b_y \tag{A.1.16}$$

$$T^y_{xz} = - T^z_{xy} \tag{A.1.17}$$

where $b_x = B_x/B$, $b_y = B_y/B$, and $b_z = B_z/B$.

D. $$(\underset{\sim}{q}^{\perp(1)} + \underset{\sim}{q}^{\parallel(1)}) \cdot \hat{x} = \frac{5}{2} \frac{p^{(0)+}}{\rho\Omega_+} \left[b_z \frac{dP^{(1)}_{xy}}{dx} - b_y \frac{dP^{(1)}_{xz}}{dx} \right] \tag{A.1.18}$$

Note that $V_x^+ \approx U$, $V_y^+ = V_y$, and $V_z^+ = V_z$ have been used.

A.2 Determination of $\delta\underset{\approx}{P}^{(1)}$ and $(\delta\underset{\sim}{q}^{\perp(1)} + \delta\underset{\sim}{q}^{\parallel(1)}) \cdot \hat{x}$ at the Stationary Points

In order to determine the shock wave train properties about the Rankine-Hugoniot stationary points, the perturbed quantities $\delta\underset{\approx}{P}^{(1)}$ and $(\delta\underset{\sim}{q}^{\perp(1)} + \delta\underset{\sim}{q}^{\parallel(1)}) \cdot \hat{x}$ are needed in terms of δB_y and δB_z . To lowest order in the perturbed variables, the coefficients of the derivatives in (A.1.8) - (A.1.18) can be taken as constant, and are to be evaluated about either the upstream or downstream flow conditions. In order to eliminate δV_y and δV_z , the perturbed form of the momentum equations (2.7) and (2.8) can be substituted

$$\frac{d\delta V_y}{dx} = \frac{B_x}{4\pi\rho U}\ \frac{d\delta B_y}{dx} - \frac{1}{\rho U}\ \frac{dP^{(1)}_{xy}}{dx} \tag{A.2.1}$$

$$\frac{d\delta V_z}{dx} = \frac{B_x}{4\pi\rho U}\ \frac{d\delta B_z}{dx} - \frac{1}{\rho U}\ \frac{dP^{(1)}_{xz}}{dx} \tag{A.2.2}$$

Since $\delta\underset{\approx}{P}^{(1)}$ is a functional of the velocity derivatives and they in turn depend on $\delta\underset{\approx}{P}^{(1)}$, to obtain $\delta\underset{\approx}{P}^{(1)}$ correct to order $(R_+/L)^2$, equations (A.1.8) - (A.1.18) must be expanded, and terms of order $(R_+/L)^3$ dropped. The calculation will be performed for $\delta P^{(1)}_{xx}$ and the results for $\delta P^{(1)}_{xy}$ and $\delta P^{(1)}_{xz}$ simply stated. Recall that $B_y = 0$ at a stationary point; hence coefficients of derivations which are proportional to B_y vanish.

Substitution of (A.2.1) and (A.2.2) into (A.1.9) yields

$$\delta T_{xx} = T^y_{xx}\left\{\frac{B_x}{4\pi\rho U}\ \frac{d\delta B_y}{dx} - \frac{1}{\rho U}\ \frac{d\delta P^{(1)}_{xy}}{dx}\right\} \tag{A.2.3}$$

where $T^z_{xx} \propto B_y = 0$ was used. Now substituting for $\delta P^{(1)}_{xy}$ from (A.1.12) and using (A.2.2) to eliminate δV_z, (A.2.3) becomes

$$\delta T_{xx} = \frac{T^y_{xx}}{4\pi\rho U}\ \frac{d\delta B_y}{dx} - \frac{T^y_{xx}\ T^x_{xy}}{\rho U}\ \frac{d^2\delta U}{dx^2}$$

$$- \frac{T^y_{xx}\ T^z_{xy}}{\rho U}\left[\frac{B_x}{4\pi\rho U}\ \frac{d^2\delta B_z}{dx^2} - \frac{1}{\rho U}\ \frac{d^2\delta P^{(1)}_{xz}}{dx^2}\right] \tag{A.2.4}$$

Since $\delta P^{(1)}_{xz}$ contains first order derivatives, the last term in (A.2.4) is of order $(R_+/L)^3$ and can be dropped, Hence $\delta P^{(1)}_{xx}$ becomes

$$\delta P_{xx}^{(1)} = \delta P^{(1)} + \frac{T_{xx}^{y} B_x}{4\pi\rho U} \frac{d\delta B_y}{dx} - \frac{T_{xx}^{y} T_{xy}^{x}}{\rho U} \frac{d^2\delta U}{dx^2} - \frac{T_{xx}^{y} T_{xy}^{z} B_x}{4\pi\rho^2 U^2} \frac{d^2\delta B_z}{dx^2} \qquad (A.2.5)$$

In order to eliminate δU in terms of δB_z, equation (3.1) after substitution of (A.2.4) for δT_{xx}, can be substituted into (A.2.5), and the result expanded to order $(R_+/L)^2$ to find

$$\delta P_{xx}^{(1)} = \delta P^{(1)} + \frac{T_{xx}^{y} B_x}{4\pi\rho U} \frac{d\delta B_y}{dx} + \left[\frac{T_{xx}^{y} T_{xy}^{x} B_z}{4\pi\rho^2 (U^2 - C_S^2)} - \frac{T_{xx}^{y} T_{xy}^{z} B_x}{4\pi\rho^2 U^2} \right] \frac{d^2\delta B_z}{dx^2} \qquad (A.2.6)$$

Similar calculations for $\delta P_{xy}^{(1)}$ and $\delta P_{xz}^{(1)}$ yield

$$\delta P_{xy}^{(1)} = \left[\frac{T_{xy}^{z} B_x}{4\pi\rho U} - \frac{T_{xy}^{x} U B_z}{4\pi\rho (U^2 - C_S^2)} \right] \frac{d\delta B_z}{dx} - \left[\frac{T_{xy}^{x} T_{xx}^{y} B_x}{4\pi\rho^2 (U^2 - C_S^2)} + \frac{T_{xy}^{z} T_{xz}^{y} B_x}{4\pi\rho^2 U^2} \right] \frac{d^2\delta B_y}{dx^2} \qquad (A.2.7)$$

$$\delta P_{xz}^{(1)} = \frac{T_{xz}^{y} B_x}{4\pi\rho U} \frac{d\delta B_y}{dx} + \left[\frac{T_{xy}^{x} T_{xz}^{y} B_z}{4\pi\rho^2 (U^2 - C_S^2)} - \frac{T_{xz}^{y} T_{xy}^{z} B_x}{4\pi\rho^2 U^2} \right] \frac{d^2\delta B_z}{dx^2} \qquad (A.2.8)$$

The ICR heat flow to order $(R_+/L)^2$ is

$$(\delta \underline{q}_{\perp}^{(1)} + \delta \underline{q}_{\perp}^{M(1)}) \cdot \hat{x} = \frac{5}{2} \frac{P^{(0)}+}{\rho\Omega_+} b_z \left[- \frac{T_{xy}^{x} U B_z}{4\pi\rho (U^2 - C_S^2)} + \frac{T_{xy}^{z} B_x}{4\pi\rho U} \right] \frac{d^2\delta B_z}{dx^2} \qquad (A.2.9)$$

ACKNOWLEDGMENTS

It is a pleasure to acknowledge many illuminating discussions with Professors W. B. Kunkel and C. F. Kennel and Drs. H. E. Petschek and R. W. Fredricks.

This research was supported in part by the National Aeronautics and Space Administration, Grant NGL-05-003-012 (Univ. Calif., Berkeley), NASA Grant NGR 05-007-190, NASA Grant NGR 05-007-116, the National Science Foundation, Grant # GP 6817, the Office of Naval Research, Grant # NONR-N00014-69-A-0200-4023, and the Atomic Energy Commission, Contract AT(11-1)-34, Project #157. (U.C.L.A.)

REFERENCES

[1] Sagdeev, R. Z., in Reviews of Plasma Physics, Vol. 4, 23, Consultants Bureau, New York, 1966.

[2] Cavaliere, A., and F. Engelmann, Nucl. Fusion, 7, 137, 1967.

[3] Camac, M., A. R. Kantrowitz, M. M. Litvak, R. M. Patrick, and H. E. Petschek, Nucl. Fusion Suppl., part 2, 423, 1962.

[4] Tidman, D.A., Phys. Fluids, 10, 547, 1967.

[5] Kennel, C.F., and R.Z.Sagdeev, J. Geophys. Res., 72, 3303, 1967.

[6] Washimi, H., and T. Taniuti, Phys. Rev. Letters, 17, 996, 1966.

[7] Montgomery, D., and G. Joyce, J. Plasma Phys., 3, 1, 1969.

[8] Biskamp, D., and D. Parkisnon, in Collision-free Shocks in the Laboratary and Space, ESRO SP-51, 191, 1969.

[9] Petschek, H. E., in Proc. AAS-NASA Symp. Phys. Solar Flares, NASA SP-50, ed. W. N. Hess, 425, Washington, D.C., 1964.

[10] Axford, W. I., H. E. Petschek, and G. L. Siscoe, J. Geophys. Res., 70, 1231, 1965.

[11] Sturrock, P., Proc. of the International School of Physics, Enrico Fermi Course XXXIX, Academic Press, 1967.

[12] Kantrowitz, A.R., and H. E. Petschek, in Plasma Physics in Theory and Application, ed. by W. B. Kunkel, 148, McGraw-Hill Book Co., New York, 1966.

[13] Coroniti, F. V., J. Plasma Phys., 4, 265, 1970a.

[14] MacMahon, A., Phys. Fluids 8, 1840, 1965.

[15] Morioka, S., and J. R. Spreiter, J. Plasma Phys., 2, 449, 1968.

[16] Schindler, K., and P. Goldberg, in Collision-free Shocks in the Laboratory and Space, ESRO SP-51, 37, 1969.

[17] Braginskii, S.I., Sov. Phys. Dokl., 2, 345, 1957.

[18] Stringer, T.E., Plasma Phys. (J. Nucl. Energy, Part C), 5, 89, 1963.

[19] Coroniti, F.V., and C.F.Kennel, J. Geophys. Res., 75, 1863, 1970.

[20] Coroniti, F.V., Thesis, Space Sciences Laboratory Series 10, Issue 36, University of California, July 1969.

[21] Formisano, V., and C. F. Kennel, J. Plasma Phys., 3, 55, 1969.

[22] Goldberg, P., to be published, Phys. Fluids, 1970.

[23] Kennel, C.F., and H.E.Petschek, in Physics of the Magnetosphere, ed. by R. L. Carovillano, J. F. McClay, and H. R. Radoski, 485, D. Reidel Publishing Co., Dordrecht, Holland, 1968.

[24] Robson, A.E., in Collision-free Shocks in the Laboratory and Space, ESRO SP-51, 159, 1969.

[25] Anderson, J.E., Magnetohydrodynamic Shock Waves, M.I.T. Press, 1963.

[26] Sarason, L., J. Math. Phys., 6, 1508, 1965.

[27] Todd, L., J. Fluid. Mech., 24, 597, 1966.

[28] Chu, C.K., and R. T. Taussig, Phys. Fluids, 10, 249, 1967.

[29] Ludford, G.S.S., J. Fluid Mech., 5, 67, 1959.

[30] Petschek, H.E., and R.M.Thorne, Astrophys. J., 147, 1157, 1967.

[31] Kinsinger, R.E., and P.L.Auer, Phys. Fluids, 12, 2580, 1969.

[32] Coroniti, F.V., submitted to Plasma Phys., 1970b.

[33] Forslund, D.W., J. Geophys. Res., 75, 17, 1970.

[34] MacMahon, A., J. Geophys. Res., 73, 7538, 1968.

FIGURE CAPTIONS

Figure 1. A sketch of a quarter quadrant of a Friedrich's diagram showing the three hydromagnetic modes for $\beta < 1$ and $\beta > 1$. Slow shocks in which the magnetic field dominates the shock structure have upstream flow velocities less than the sound speed C_S; in MHD resistivity alone provides the required dissipation. Slow shocks with upstream flow velocities exceeding C_S should in a collisionless plasma be primarily electrostatic; in MHD viscous dissipation is needed for a shock transition. NE = non-evolutionary range of flow velocities for slow shocks.

Figure 2. In the upper half of the figure the spatial wave train structure of the tangential magnetic field for a low-β magnetic slow switch-off shock is sketched against distance through the shock. The magnetic field undergoes rotations in direction with a wavelength $\sim c/\omega_{p_+}$ while the magnetic field magnitude decreases slowly with a scale length $\sim c^2/\omega_{p_+}^2 \; r_m$. An "end-on" view of the magnetic rotational structure is included. The magnetic rotations are almost incompressible so that the density variation through the shock is very gradual.

Figure 3. The scale length of the leading edge magnetic field gradient for low-β magnetic slow shocks is sketched against the slow shock Mach number. The scale length initially decreases with increase M_{SL}. However, as the switch-off shock limit is approached, the scale length increases until the steepening length is limited by magnetic resistive diffusion.

MAGNETIC SLOW SHOCKS RANGE OF UPSTREAM FLOW VELOCITIES

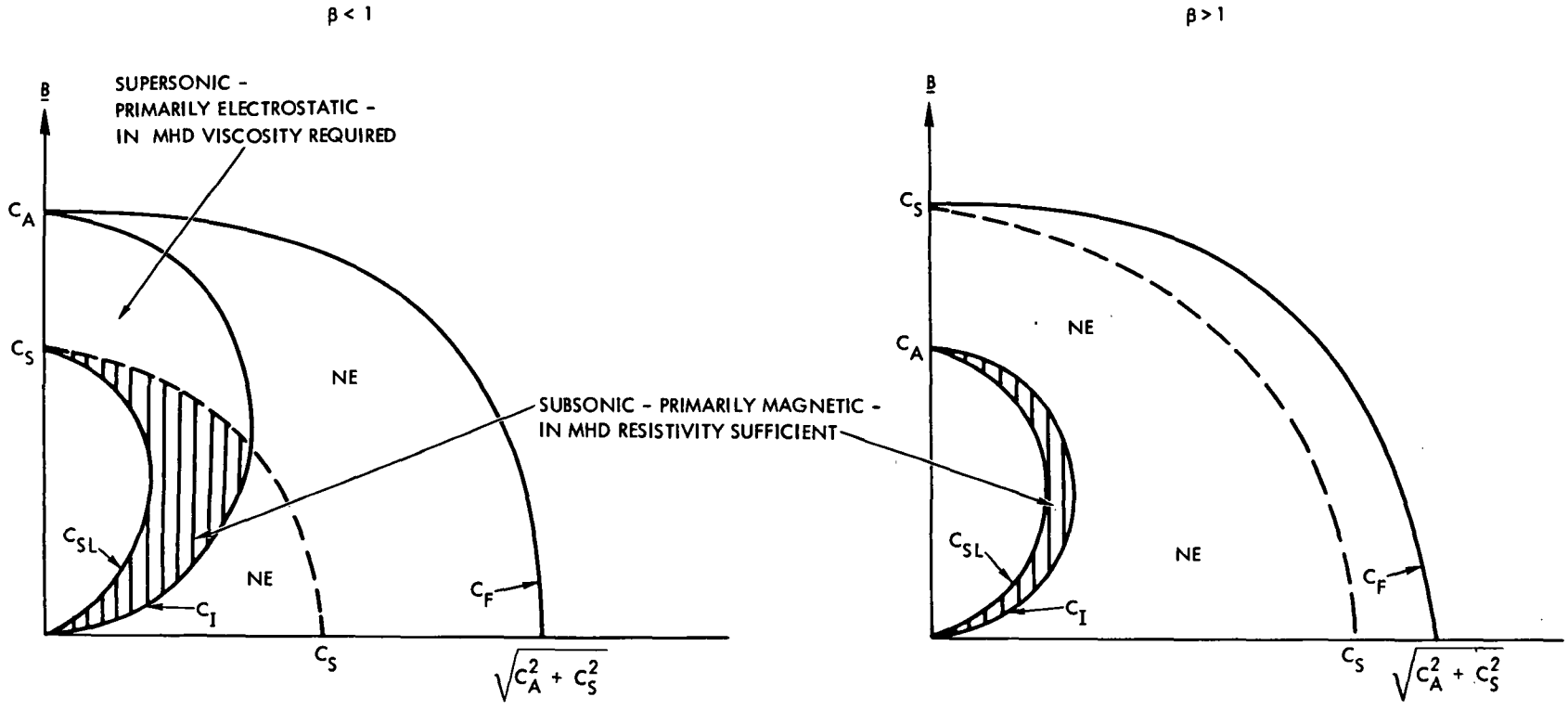

SLOW MAGNETIC SWITCH - OFF SHOCK WAVE TRAIN STRUCTURE

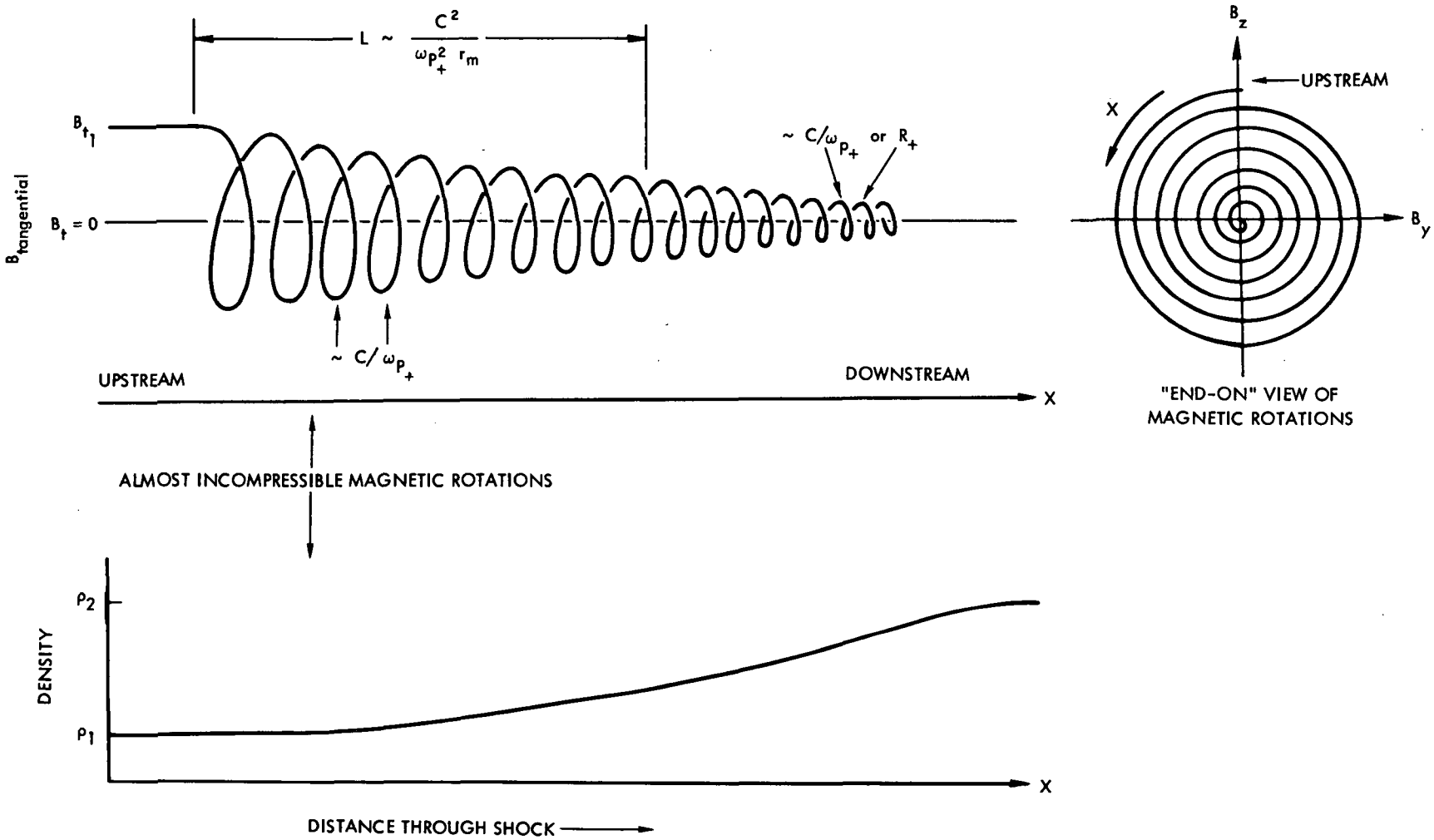

SCALE LENGTH OF LEADING EDGE MAGNETIC GRADIENT VS M_{SL} FOR LOW-β MAGNETIC SLOW SHOCKS